

Three-Nucleon Force Effects in Nucleon Induced Deuteron Breakup: Comparison to Data (II)

J. Kuroś-Żołnierczuk¹, H. Witała¹, J. Golak^{1,2}, H. Kamada³, A. Nogga⁴, R. Skibiński¹,
W. Glöckle²

¹*M. Smoluchowski Institute of Physics, Jagiellonian University, Reymonta 4, 30-059 Kraków,
Poland*

²*Institut für Theoretische Physik II, Ruhr Universität Bochum, D-44780 Bochum, Germany*

³*Department of Physics, Faculty of Engineering, Kyushu Institute of Technology
1-1 Sensucho, Tobata, Kitakyushu 804-8550, Japan*

⁴*Department of Physics, University of Arizona, Tucson, Arizona, 85721, USA*

(November 3, 2018)

Abstract

Selected Nd breakup data over a wide energy range are compared to solutions of Faddeev equations based on modern high precision NN interactions alone and adding current three-nucleon force models. Unfortunately currently available data probe phase space regions for the final three nucleon momenta which are rather insensitive to 3NF effects as predicted by current models. Overall there is good to fair agreement between present day theory and experiment but also some cases exist with striking discrepancies. Regions in the phase space are suggested where large 3NF effects can be expected.

21.30.-x, 21.45.+v, 25.10.+s, 24.70.+s

I. INTRODUCTION

In a previous paper [1], called I in the following, we performed a systematic search for 3NF effects in the full phase space of the Nd breakup process. To that aim we determined the predictions for the five-fold differential breakup cross section and several analyzing powers based on the current high-precision NN potentials AV18 [2], CD Bonn [3], Nijm I, II and Nijm 93 [4] alone. These predictions form a band for each of the observables as a function of the five variables needed for a kinematically complete determination of the breakup process. These five variables define a point in the phase space. Then we added to each of the five NN potentials the Tucson-Melbourne three-nucleon force (TM 3NF) [5,6] which, with the help of a strong form factor parameter, has been adjusted to the ^3H binding energy separately for each NN force [7]. The predictions for the observables based on these force combinations form another band. We talk of 3NF effects if the two bands are significantly separated. In addition we regarded two special cases, the NN and 3NF combinations AV18 + Urbana IX [8] and CD Bonn + TM', where TM' is a modified TM 3NF, which corrects a violation of chiral symmetry in TM [9,10]. All the studies have been carried through with fully converged solutions of the Faddeev equations for four nucleon laboratory energies: 13, 65, 135 and 200 MeV. In this manner we covered a wide range of energies and could identify the different phase space regions, where for each of the observables 3NF effects, based on the current models, can be expected. It is now the aim of this paper to compare our predictions with existing data. Unfortunately, in contrast to Nd elastic scattering, where precise data are numerous (see references in I), the existing data base for the breakup process is much less numerous, especially at higher energies. Unfortunately, as we shall see, the phase space regions, where the current models predict large 3NF effects, have not yet been explored experimentally.

Here we can not display all the existing data. For references to older data (before 1980) we refer to [11]. We also have to omit a very interesting full phase space search [12]. Unfortunately the access to the data is no longer possible and the documentation in [12] is insufficient to analyse the data newly. At that time they were analysed based on pioneering calculations by Kloet and Tjon [13]. They used very simple spin dependent S -wave forces, which are highly insufficient by present day standards. Moreover those data had a high statistical error. Therefore we are looking forward to the data currently being taken at KVI Groningen [14,15], which will cover a large part of the phase space, too, and will be much more accurate.

In Section II we present a comparison of our theoretical predictions with a selection of more recent breakup data (after 1980). Most of them have been analyzed before by us [11] choosing either older NN potentials (Bonn B, AV14, Paris) or only one of the modern ones. Also the addition of 3NFs has not been performed before to such an extent as in this paper. The criteria for the selection of data are, that no averaging according to acceptances and angular openings have to be performed, well documented data are available and the experimental errors are small. ¹ Further we favored cases where the same observables were measured by different groups and we tried to cover the total phase space as much as possible.

¹Because of lack of other data we had to include some with large error bars.

For other data known to us (after 1980) and not shown we provide at least references. We close with a brief summary in Section III.

II. COMPARISON TO THE DATA

There are obviously continuously varying breakup configurations and the experimental groups had to make a choice. Up to now so called specific configurations like FSI, QFS, STAR, and COLL have mostly been measured. Their meaning will be explained below together with the discussion of the data. We have chosen data at 13 MeV representing the low energy region and at 65 MeV for the higher energy region. Recently new data appeared at 200 MeV [17], which we will also show.

As described in the introduction our theoretical predictions will be displayed in form of two bands corresponding to NN forces only and adding the TM 3NF. In addition there will be two curves for the combinations AV18 + Urbana IX and CD Bonn + TM'.

A. Energy 13 MeV

The majority of the breakup experiments were performed in the region of low energies ($\lesssim 25$ MeV) for both the nd [18–26] and the pd [27–36] breakup. We compare some of the 13 MeV data with our theoretical predictions for the cross section and nucleon analyzing power A_y in Figs. 1 and 12.

Let us first regard the cross sections which are given at the following special configurations: the quasi-free scattering (QFS) geometry, where one of the nucleons in the final state is at rest in the laboratory frame; the final state interaction (FSI) geometry, where the relative energy of two outgoing nucleons is equal to zero; the coplanar STAR geometry, where the three nucleons emerge from the reaction in the c.m. system with coplanar and equal momenta at 120° relative to each other and where the beam lies in that plane and also the symmetric space STAR (SSS) geometry, where the c.m. plane containing the nucleon momenta is perpendicular to the beam direction; the collinear (COLL) configuration, where one of the nucleons is at rest in the c.m. system and therefore the other two have momenta back to back. In addition two unspecific configurations have been chosen in Figs. 7 and 8.

As is seen in Figs. 1-8 the two bands are only slightly shifted to each other and therefore 3NF effects are very small at this energy. The pure 2N force predictions agree in many cases with the data.

Especially interesting is the SSS configuration for which pd [28] as well as nd data taken by different groups [18,21,23] exist. For this configuration our theoretical nd predictions shown in Fig. 4 underestimate the nd data by about 20% and overestimate the pd data by about 15%. The discrepancy for the pd data could probably have its origin in the neglected pp Coulomb force. The origin of the difference to the nd data, called the *space star anomaly* [23], is still unknown. The disagreement here is quite surprising, since the calculations [22] show that the NN S -wave contributions are the dominant part in the space

star geometry ² and their properties are rather well determined in the NN system.

The example with an FSI interaction peak shown in Fig. 2 is also very interesting. This type of peak can be used to extract np or nn scattering lengths (a_{np} or a_{nn}) in the state 1S_0 . In such a manner the well known a_{np} could be extracted with the correct value using only NN forces [25,26,37]. In case of a_{nn} there exists a challenging controversy, where two independent nd breakup measurements lead to quite different results [25,37]. One [37] agrees with the usually quoted value found in the π^-d absorption process, while the other one [25] is significantly smaller in magnitude.

We also display a coplanar STAR result, where a renewed measurement [21] agrees quite well with present day nuclear force predictions now, while an older one [18] is far off. A corresponding shift of data occurred also for the COLL configuration $(\theta_1, \theta_2, \phi_{12}) \equiv (39^\circ, 75.5^\circ, 180^\circ)$, where the new data [21] agree with theory in contrast to the old one [18].

But there are also discrepancies. One example of QFS condition is shown in Fig. 1. It is unknown, whether pp Coulomb force corrections are responsible for those deviation. A more recent measurement [38] also shows the discrepancy for QFS conditions. Very remarkable is also that in one of the two unspecific configurations $(17^\circ, 50.5^\circ, 120^\circ)$ we see a dramatic disagreement of theory and data. A remeasurement would be highly welcome.

For the nucleon analyzing power A_y , the agreement to NN force predictions alone is, in general, good (see Figs. 9-12), though, the data scatter and have large error bars. All 3NFs give small effects for this observable in the chosen configurations at this energy.

Further data in the low energy region can be found in [11]. The agreement with theory is similar as for the selected examples shown, with some further exceptions in the data set from Erlangen [18,20] and [36].

Now, regarding the information gained in I, one has to ask whether the available data probed the phase space regions, where current 3NF models predict significant effects. The answer is unfortunately no. For the breakup cross section the sensitive regions to see 3NF effects at 13 MeV are around $\theta_1 = \theta_2 = 50^\circ$ and $\phi_{12} = 170^\circ$. Data there would be very useful. For the analyzing power A_y corresponding sensitive regions are around $\theta_1 = 100^\circ$, $\theta_2 = 30^\circ$ (and vice versa) and $\phi_{12} = 160^\circ$. Unfortunately in this case the proton energies are rather small (≤ 3 MeV).

B. Energy 65 MeV

At this energy the five-fold differential cross section and the proton analyzing power were measured for the $\vec{d}(p, pp)n$ reaction in 13 different kinematically complete configurations [39–41]. In FIGS. 13-25 those data are compared to our theoretical predictions.

Let us first regard the cross sections. In cases where the two bands are narrow and either overlap or are close together the agreement with the data is rather good, with the exception of the two QFS configurations (see FIGS. 16,17), a backward plane star (BPS) configuration (see Fig. 15), and an unspecific one $(20^\circ, 116.2^\circ, 0^\circ)$ (see Fig. 25). The BPS

²60% of the space star cross section is due to the 3S_1 NN force, 30% due to the 1S_0 force and only about 10% comes from the P -wave forces [22].

configuration denotes the situation where one of the three nucleons goes antiparallel to the beam direction. There is also forward plane star (FPS) configuration where one of the nucleons goes along the beam direction. Note in all cases one should keep in mind that the magnitude of the pp Coulomb force effects under the different conditions are not known. For the QFS configurations one might indeed expect small 3NF effects, as we see, since by definition of that configuration one final nucleon is at rest and thus in a simple picture is like a spectator to a two-nucleon process. This is, however, not quite right, since that "spectator nucleon" is heavily rescattered as a comparison of the full solution with a plane wave assumption for that nucleon reveals [11,42]. Our results show that, 3NF effects remain thereby small. As we have seen at 13 MeV and what we found at other energies below about 25 MeV, theory overshoots the experimental QFS maxima by about 20%. This decreases but remains still significant at 65 MeV with about 13%. Also the QFS peak at 65 MeV is narrower than the theory predicts. All that might suggest again Coulomb force effects to be mostly responsible for the discrepancies. There are indeed first steps (based on low rank NN forces) which point to quite large Coulomb force effects for the breakup cross section [43].

In the two cases in Fig. 13 and 19 where the two bands are distinct (say larger than 10%) the situation is controversial. In one case (SSS) NN predictions alone touch at least the error bars but 3NFs move theory away from the data. In the other case, a COLL one, neither NN forces alone nor the addition of 3NFs leads to an agreement with the data.

Like at 13 MeV the SSS configuration poses a question. It has been measured at several energies. In all cases the pd data lie below the theoretical predictions, but this discrepancy decreases with increasing energy (about 15% at 10.5 MeV [19,20] and 13 MeV and about 7% at 19 MeV [29] and 65 MeV). Because of that decrease and the relative small 3NF effects one faces possibly again pp Coulomb force effects.

For A_y , like for σ , in the cases where the two bands are narrow and essentially overlapping there is agreement with the data with the exception of the configuration $(59.5^\circ, 59.5^\circ, 180^\circ)$ (see Fig. 21), where theory is partially below and partially above the data. When the bands are wider and clearly distinct unfortunately the data scatter a lot (see the configurations $(30^\circ, 59.5^\circ, 180^\circ)$ -Fig.16, $(20^\circ, 116.2^\circ, 180^\circ)$ -Fig.18, $(30^\circ, 98^\circ, 180^\circ)$ -Fig.19). There are two more cases with less narrow bands ($(45^\circ, 75.6^\circ, 180^\circ)$ -Fig.20 and $(20^\circ, 75.6^\circ, 180^\circ)$ -Fig.24), where the data appear to differ from theory.

Further breakup data at and around 65 MeV can be found in [30,39–41,44–47].

Again we ask, whether the sensitive regions for 3NF effects according to I have been included in the existing data base. Unfortunately this is again not the case. The sensitive regions for the cross section and A_y are around $\theta_1 \sim 20^\circ, \theta_2 \sim 10^\circ$ (and vice versa) and $0^\circ \leq \phi_{12} \leq 60^\circ$. Though the configuration $(30^\circ, 98^\circ, 180^\circ)$, for instance, in case of A_y shows an interesting sensitivity to 3NFs, the effects are only of 30%, whereas effects of up to 100% and higher are predicted in the geometries just mentioned.

C. Energy 200 MeV

In Figs. 26-33 we show a comparison of our theoretical predictions with the pd data of [17] for the cross section $\frac{d^3\sigma}{d\Omega_1 d\Omega_2 dE_1}$ and the nucleon analyzing power A_y . For the cross section the two bands are very narrow and overlapping. Thus we predict practically no 3NF effects. It is no surprise, since most of the configurations are in the vicinity of QFS. The comparison

with the data, however, shows striking disagreements in most cases. Though the shapes are generally quite well reproduced, the magnitudes are wrong. This is alarming, since the current nuclear forces fail strongly. Note, however, we have no estimate for relativistic effects, which at this high energy can contribute both kinematically and dynamically.

Also in case of A_y the two bands are mostly rather narrow and overlapping. Since some of the data have large error bars, agreement or disagreement of theory and data is not clear.

We are not aware of other breakup data in that energy region. The sensitive regions for 3NF effects are around $\theta_1 \sim 15^\circ \sim \theta_2$ and $0^\circ \leq \phi_{12} \leq 20^\circ$ for the cross section and $\theta_1 \sim 100^\circ$, $\theta_2 \sim 30^\circ$ (and vice versa) and $\phi_{12} \sim 180^\circ$ for A_y .

III. SUMMARY

We compared modern NN force predictions alone and together with current 3NF models to a selected set of Nd breakup cross sections and analyzing power data at 13, 65 and 200 MeV. Though in most cases the agreement was good, we also found cases with striking discrepancies between theory and experiment. The discrepancies showed up in the SSS, QFS and some unspecified geometries at low energies. Severe discrepancies are also present in the cross sections at 200 MeV. In all those cases the 3NF effects predicted by the current models are very small. At 200 MeV we can not exclude that at least one reason for the discrepancy might lie in the totally neglected relativistic effects. At the lower energies pp Coulomb effects, not included in our theoretical description, might also play a role. In case of the analyzing power A_y we found some discrepancies at 65 MeV, which point to deficiencies in the current nuclear force models. Some configurations with interesting theoretical 3NF effects at this energy could not be checked conclusively against experiment, since there is a big scatter in the available data.

The experiments performed so far show that it is rather difficult to find by chance a configuration with large 3NF effects. Therefore the breakup experiments should be guided by theoretical predictions like the one in I. Also the present day Nd breakup data set is much poorer than the elastic scattering one, what calls for more data. Especially cross section and analyzing power measurements at higher energies in configurations where large 3NF effects have been predicted are highly desirable.

ACKNOWLEDGMENTS

This work was supported by the Polish Committee for Scientific Research (Grant No. 2P03B02818 and 5P03B12320), the Deutsche Forschungsgemeinschaft (J.G.), and the NSF (Grant No. PHY0070858). One of us (W.G.) would like to thank the Foundation for Polish Science for the financial support during his stay in Cracow. The numerical calculations have been performed on the Cray T90 and T3E of the NIC in Jülich, Germany.

REFERENCES

- [1] J. Kuroś-Żołnierczuk, H. Witała, J. Golak, H. Kamada, A. Nogga, R. Skibiński, W. Glöckle, submitted for publication in Phys. Rev. C.
- [2] R. B. Wiringa, V. G. J. Stoks, R. Schiavilla, Phys. Rev. **C51**, 38 (1995).
- [3] R. Machleidt, F. Sammarruca, and Y. Song, Phys. Rev. **C53**, R1483 (1996).
- [4] V. G. J. Stoks, R. A. M. Klomp, C. P. F. Terheggen, J. J. de Swart, Phys. Rev. **C49**, 2950 (1994).
- [5] S. A. Coon *et al.*, Nucl. Phys. **A317**, 242 (1979).
- [6] S. A. Coon, W. Glöckle, Phys. Rev. **C23**, 1790 (1981).
- [7] A. Nogga, H. Kamada, and W. Glöckle, Phys. Rev. Lett. **85**, 944 (2000).
- [8] B. S. Pudliner, V. R. Pandharipande, J. Carlson, S. C. Pieper, and R. B. Wiringa, Phys. Rev. **C56**, 1720 (1997).
- [9] J. L. Friar, D. Hüber, U. van Kolck, Phys. Rev. **C59**, 53 (1999).
- [10] D. Hüber, J. L. Friar, A. Nogga, H. Witała, U. van Kolck, Few-Body Syst., **30**, 95 (2001).
- [11] W. Glöckle, H. Witała, D. Hüber, H. Kamada and J. Golak, Phys. Rep. **274**, 107 (1996).
- [12] G. J. F. Blommestijn, R. van Dantzig, Y. Haitzma, R. B. M. Mooy, I. Slaus, Nucl. Phys. **A365**, 202 (1981).
- [13] W. M. Kloet, J. A. Tjon, Nucl. Phys. **A210**, 380 (1973); Ann. Phys. **79**, 407 (1973).
- [14] St. Kistryn *et al.*, Nucl. Phys. **A689**, 345c (2001).
- [15] K. Bodek, private communication.
- [16] R. Bieber *et al.*, Nucl. Phys. **A684**, 536c (2001).
- [17] W. Pairsuwan *et al.*, Phys. Rev. **C52**, 2552 (1995).
- [18] J. Strate *et al.*, Nucl. Phys. **A501**, 51 (1989).
- [19] M. Stephan *et al.*, Phys. Rev. **C39**, 2133 (1989).
- [20] K. Gebhardt *et al.*, Nucl. Phys. **A561**, 232 (1993).
- [21] C. Howell *et al.*, Nucl. Phys. **A631**, 692c (1998).
- [22] H. Setze *et al.*, AIP Conf. Proc. **334**, 463 (1995).
- [23] H. Setze *et al.*, Phys. Lett. **B388**, 229 (1996).
- [24] W. Tornow *et al.*, Few-Body Syst. Suppl. **8**, 163 (1995).
- [25] V. Huhn *et al.*, Phys. Rev. Lett. **85**, 1190 (2000).
- [26] V. Huhn *et al.*, Phys. Rev. **C63**, 014003 (2001).
- [27] F. Correll *et al.*, Nucl. Phys. **A475**, 407 (1987).
- [28] G. Rauprich *et al.*, Nucl. Phys. **A535**, 313 (1991).
- [29] H. Patberg *et al.*, Phys. Rev. **C53**, 1497 (1996).
- [30] L. Qin *et al.*, Nucl. Phys. **A587**, 252 (1995).
- [31] F. Foroughi *et al.*, Nucl. Phys. **A346**, 139 (1980).
- [32] M. Karus *et al.*, Phys. Rev. **C31**, 1112 (1985).
- [33] M. Przyborowski *et al.*, Phys. Rev. **C60**, 064004 (1999).
- [34] H. Paetz gen. Schieck *et al.*, Few-Body Syst. **30**, 81 (2001).
- [35] R. Grossmann *et al.*, Nucl. Phys. **A603**, 161 (1996).
- [36] M. Zadro *et al.*, Il Nuovo Cimento **107A**, 185 (1994).
- [37] D. E. González Trotter *et al.*, Phys. Rev. Lett. **83**, 3788 (1999).
- [38] W. von Witsch, private communication.
- [39] M. Allet *et al.*, Phys. Rev. **C50**, 602 (1994).

- [40] J. Zejma *et al.*, Phys. Rev. **C55**, 42 (1997).
- [41] K. Bodek *et al.*, Few-Body Syst. **30**, 65 (2001).
- [42] H. Witała, W. Glöckle and Th. Cornelius, Few-Body Syst. **6**, 79 (1989).
- [43] E. Alt and M. Rauh, Few-Body Syst. **17**, 121 (1994).
- [44] M. Allet *et al.*, Few-Body Syst. Suppl. **7**, 243 (1994).
- [45] M. Allet *et al.*, Few-Body Syst. **20**, 27 (1996).
- [46] M. Allet *et al.*, Few-Body Syst. Suppl. **8**, 49 (1996).
- [47] D. A. Low *et al.*, Phys. Rev. **C44**, 2276 (1991).

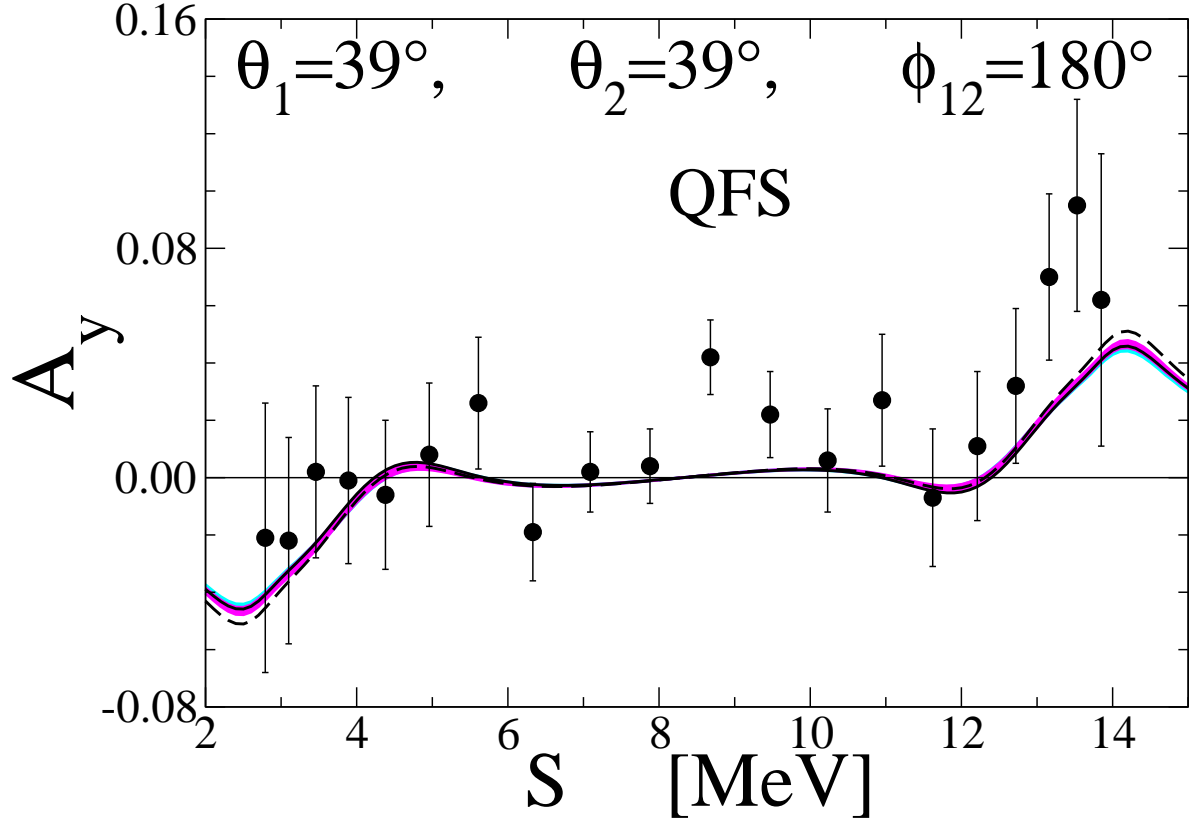


FIG. 1. Nd breakup cross section data in $[\text{mb MeV}^{-1}\text{sr}^{-2}]$ at 13 MeV in comparison to NN force predictions alone (light shaded band) and adding the TM 3NF (dark shaded band); further shown is CD Bonn + TM' (dashed line) and AV18 + Urbana IX (solid line). The pd data (full circles) are from [28].

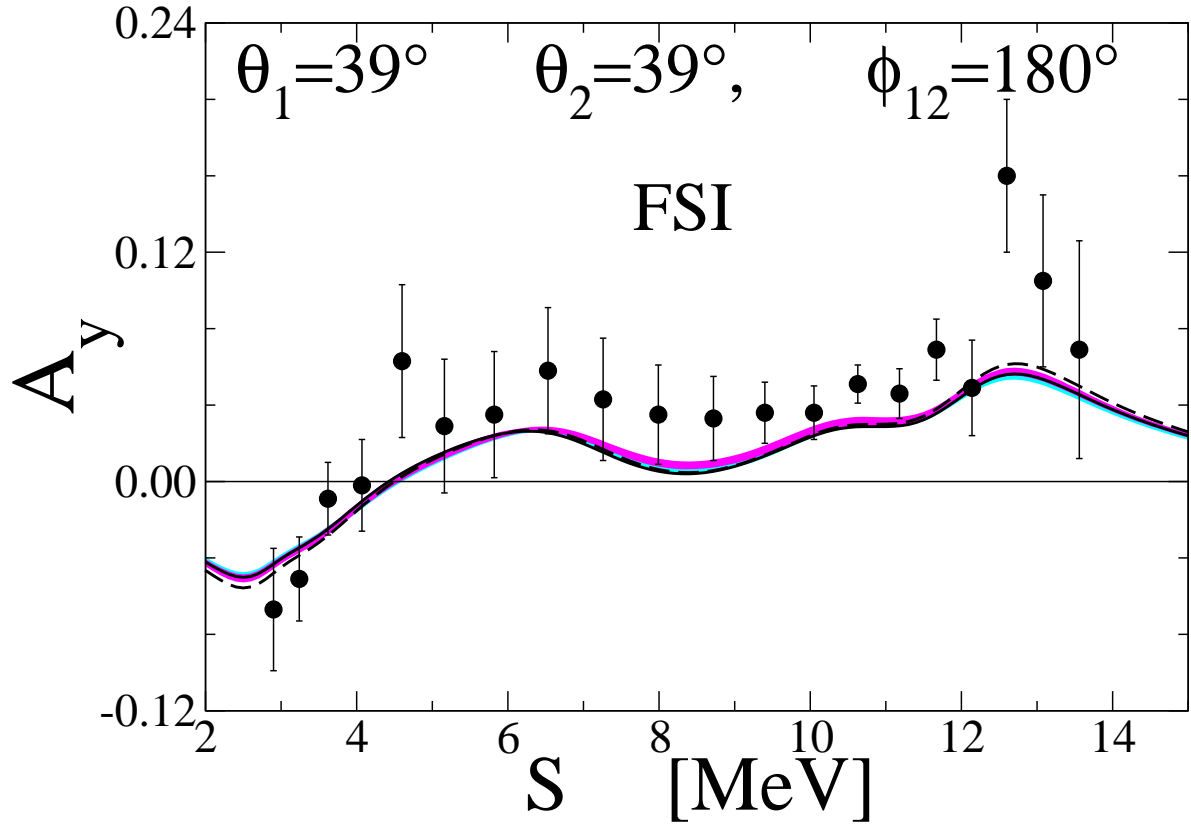


FIG. 2. Nd breakup cross section data in $[\text{mb MeV}^{-1}\text{sr}^{-2}]$ at 13 MeV in comparison to theoretical predictions. Bands and curves as in 1. The nd data are from [21] (stars), [18] (open circles), and the pd data from [28] (full circles).

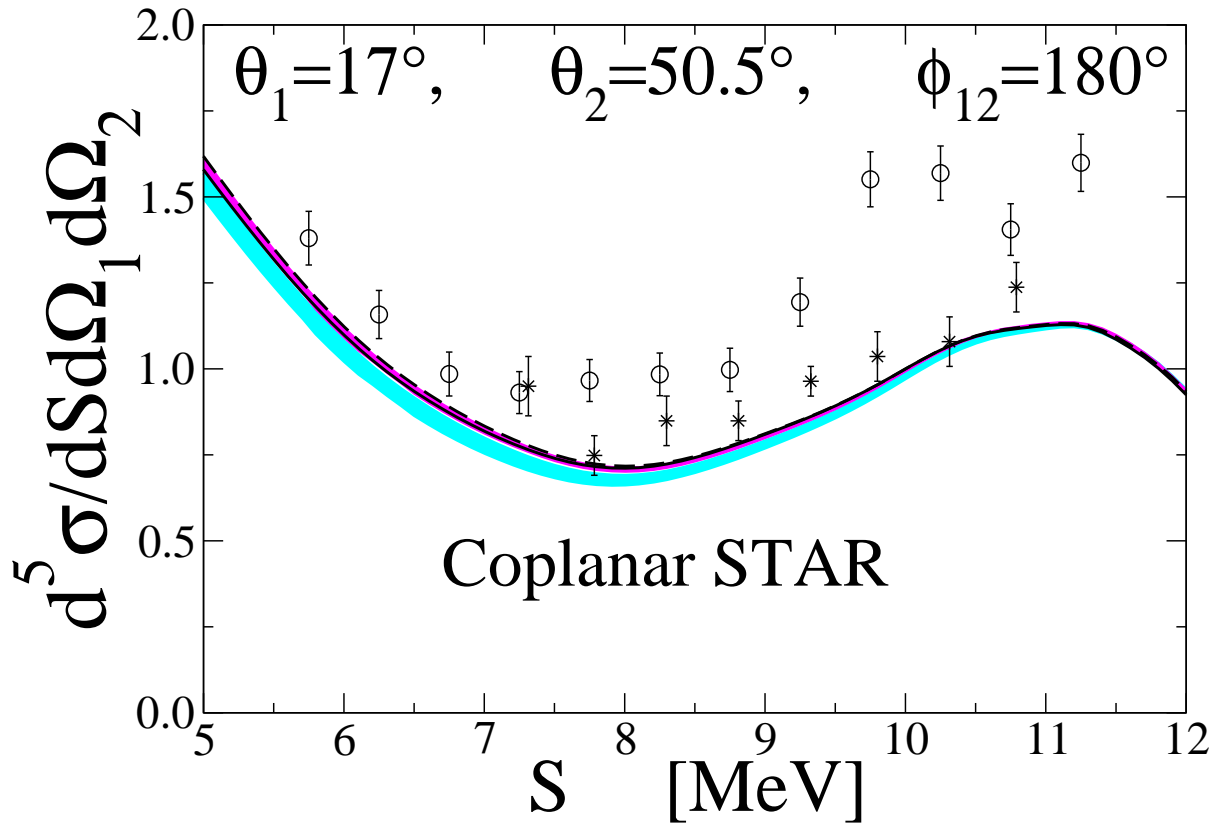


FIG. 3. Nd breakup cross section data in $[\text{mb MeV}^{-1} \text{sr}^{-2}]$ at 13 MeV in comparison to theoretical predictions. Bands and curves as in 1. The nd data are from [21] (stars) and [18] (open circles).

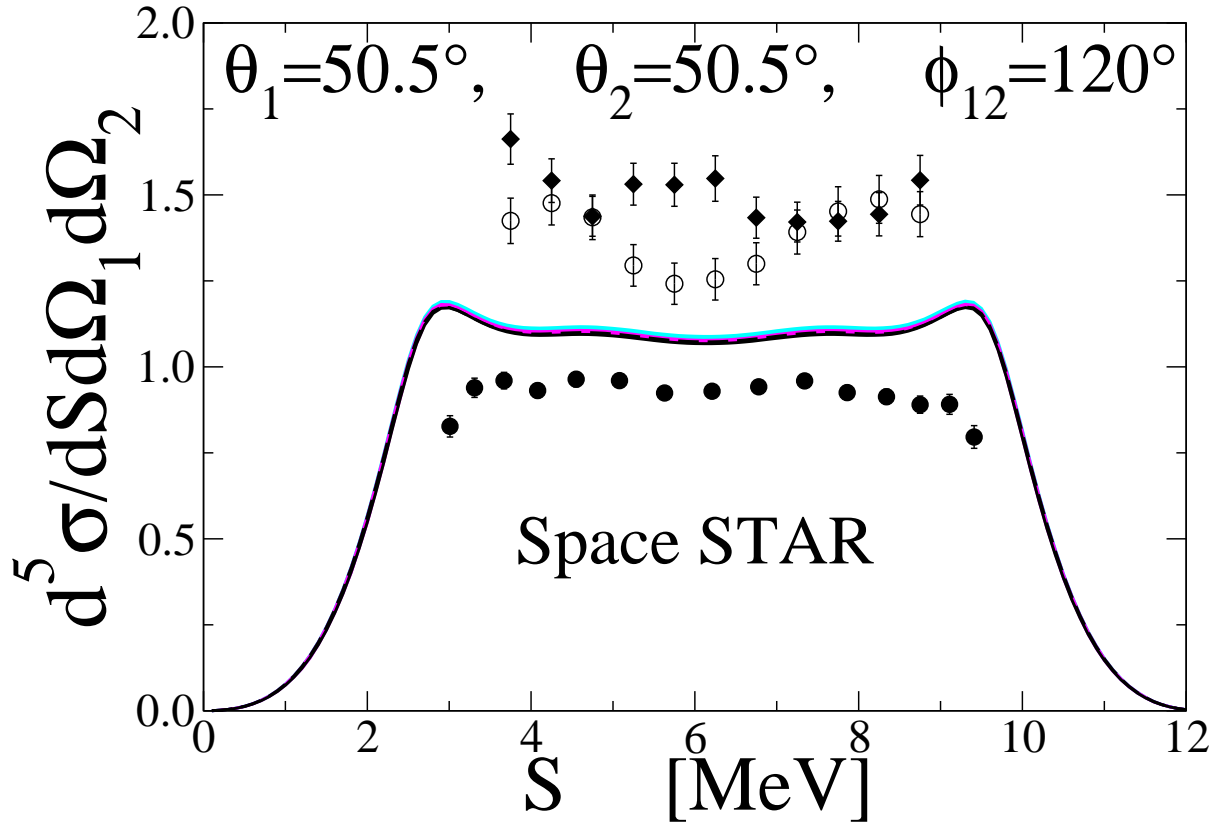


FIG. 4. Nd breakup cross section data in $[\text{mb MeV}^{-1}\text{sr}^{-2}]$ at 13 MeV in comparison to theoretical predictions. Bands and curves as in 1. The nd data are from [18] (open circles), [23] (full diamonds) and the pd data from [28] (full circles).

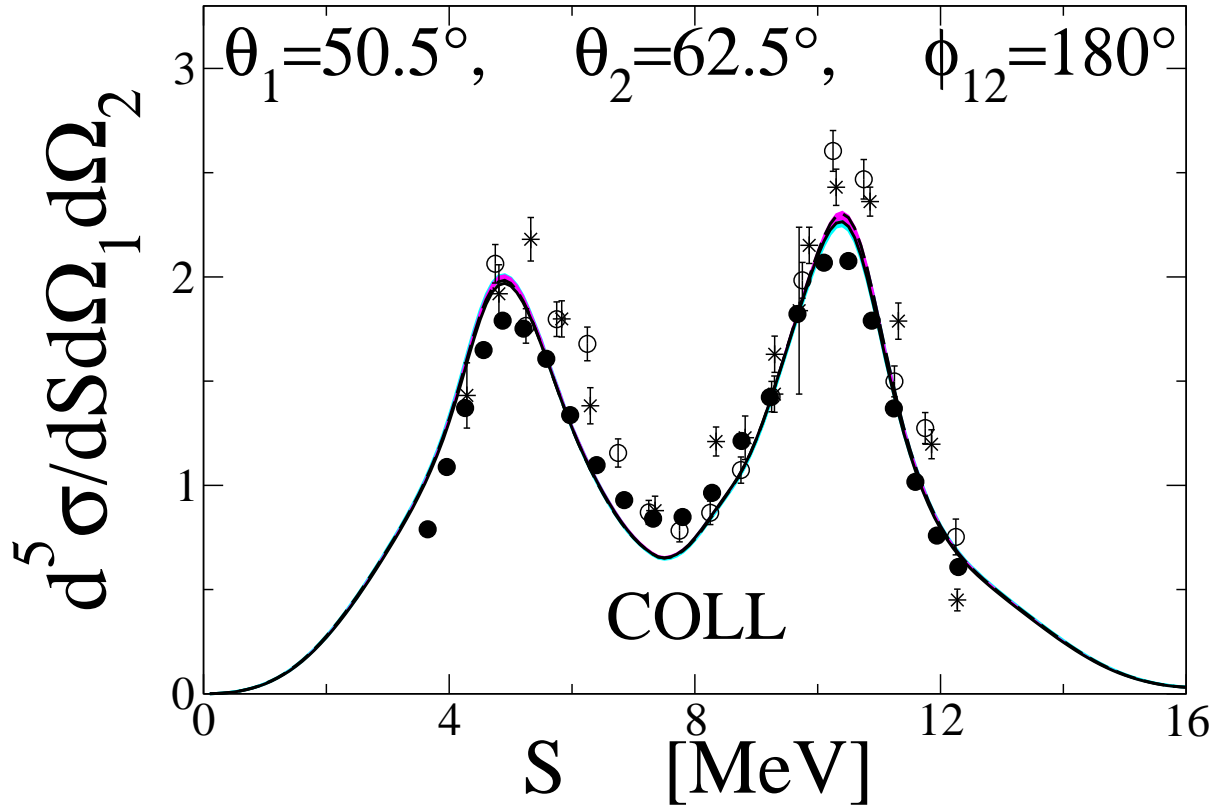


FIG. 5. Nd breakup cross section data in $[\text{mb MeV}^{-1}\text{sr}^{-2}]$ at 13 MeV in comparison to theoretical predictions. Bands and curves as in 1. The nd data are from [18] (open circles), [18] (open circles), and the pd data from [28] (full circles).

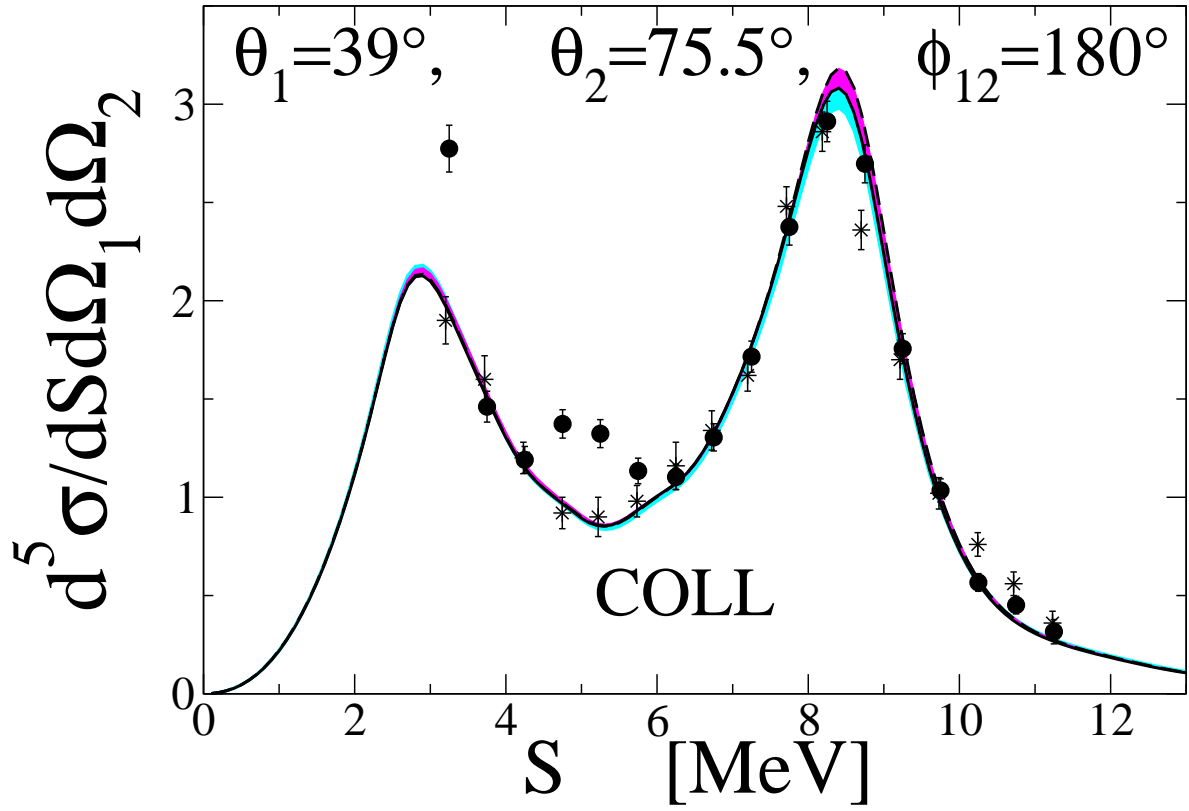


FIG. 6. Nd breakup cross section data in $[\text{mb MeV}^{-1}\text{sr}^{-2}]$ at 13 MeV in comparison to theoretical predictions. Bands and curves as in 1. The nd data are from [21] (stars) and the pd data from [28] (full circles).

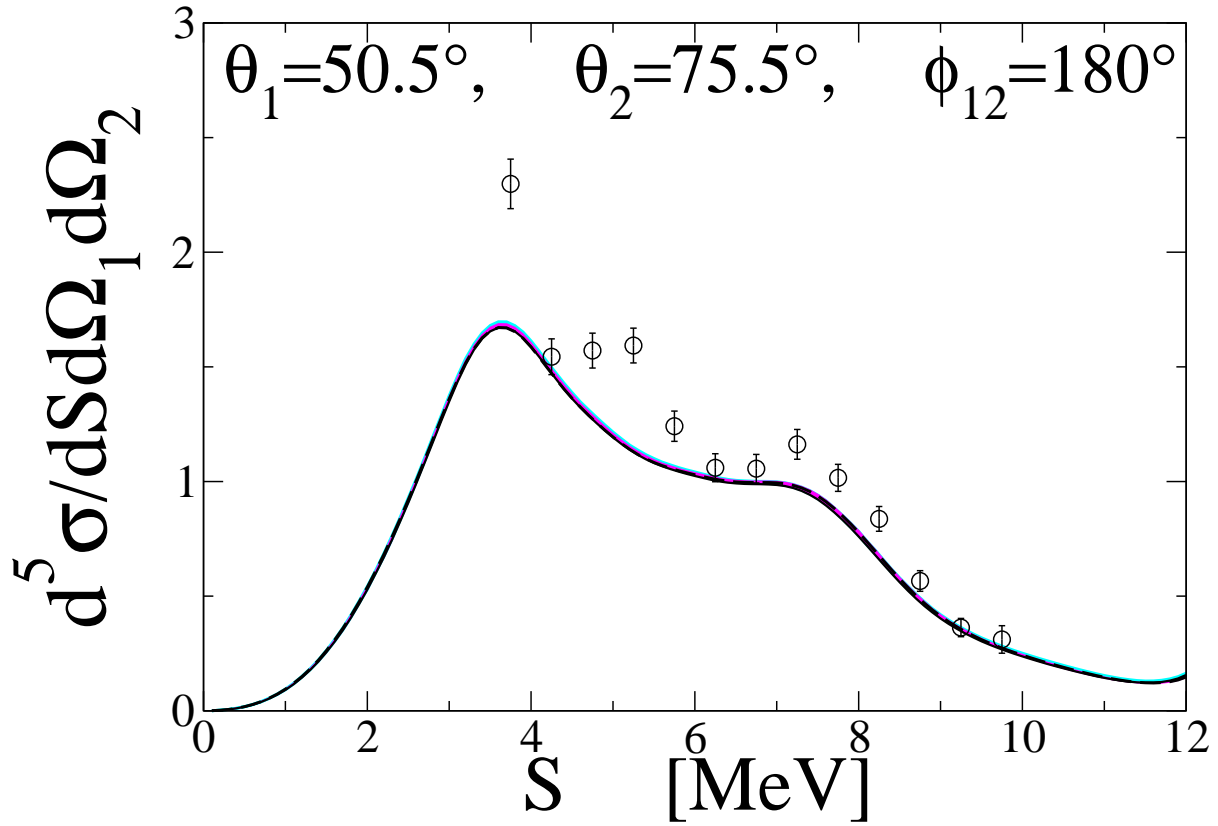


FIG. 7. Nd breakup cross section data in $[\text{mb MeV}^{-1} \text{sr}^{-2}]$ at 13 MeV in comparison to theoretical predictions. Bands and curves as in 1. The nd data are from [18].

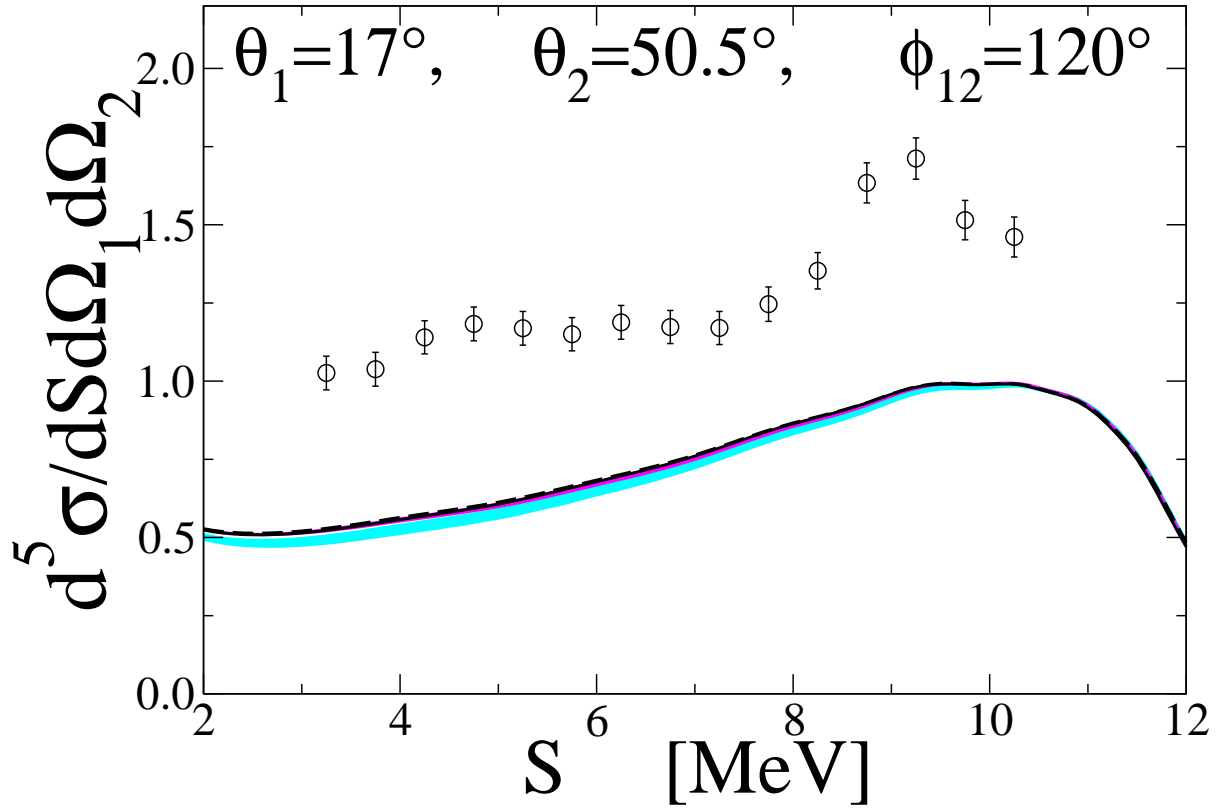


FIG. 8. Nd breakup cross section data in $[\text{mb MeV}^{-1} \text{sr}^{-2}]$ at 13 MeV in comparison to theoretical predictions. Bands and curves as in 1. The nd data are from [18].

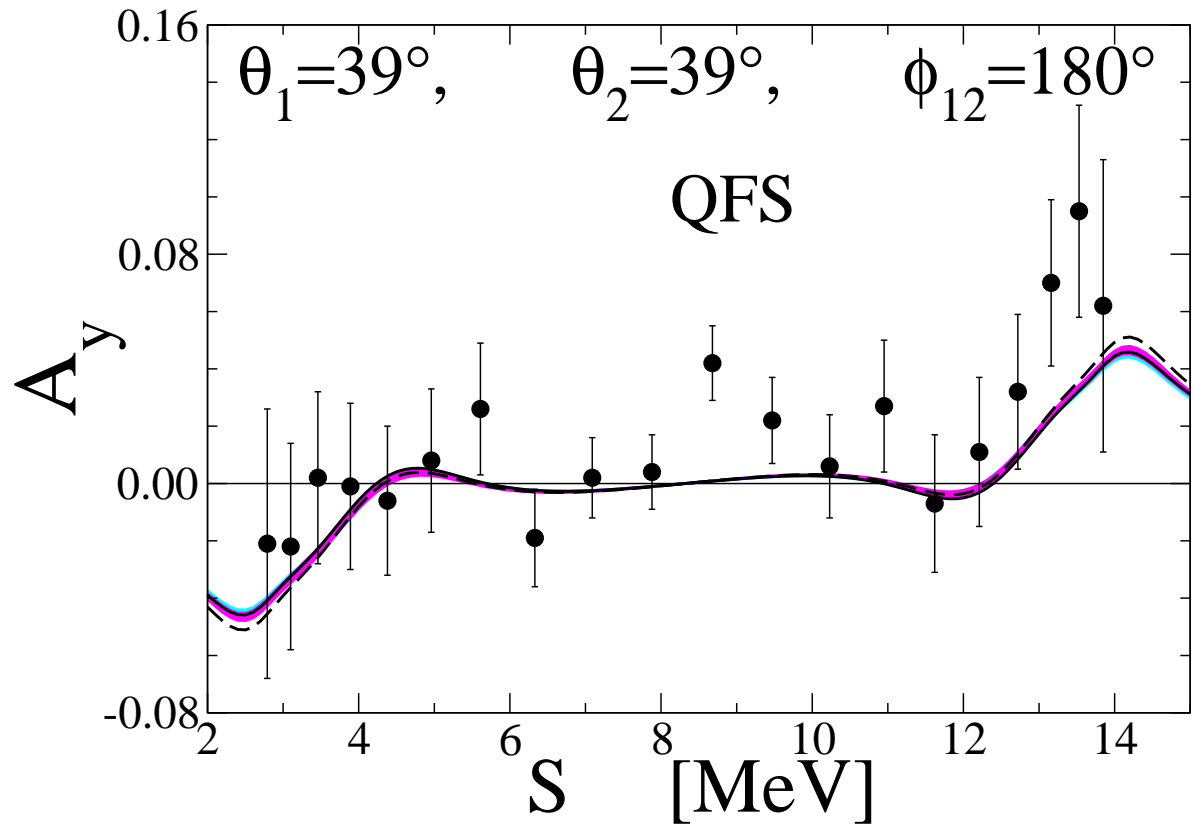


FIG. 9. Nucleon analyzing power A_y data in Nd breakup at 13 MeV in comparison to theory. Bands and curves as in Fig. 1. The pd data are from [28].

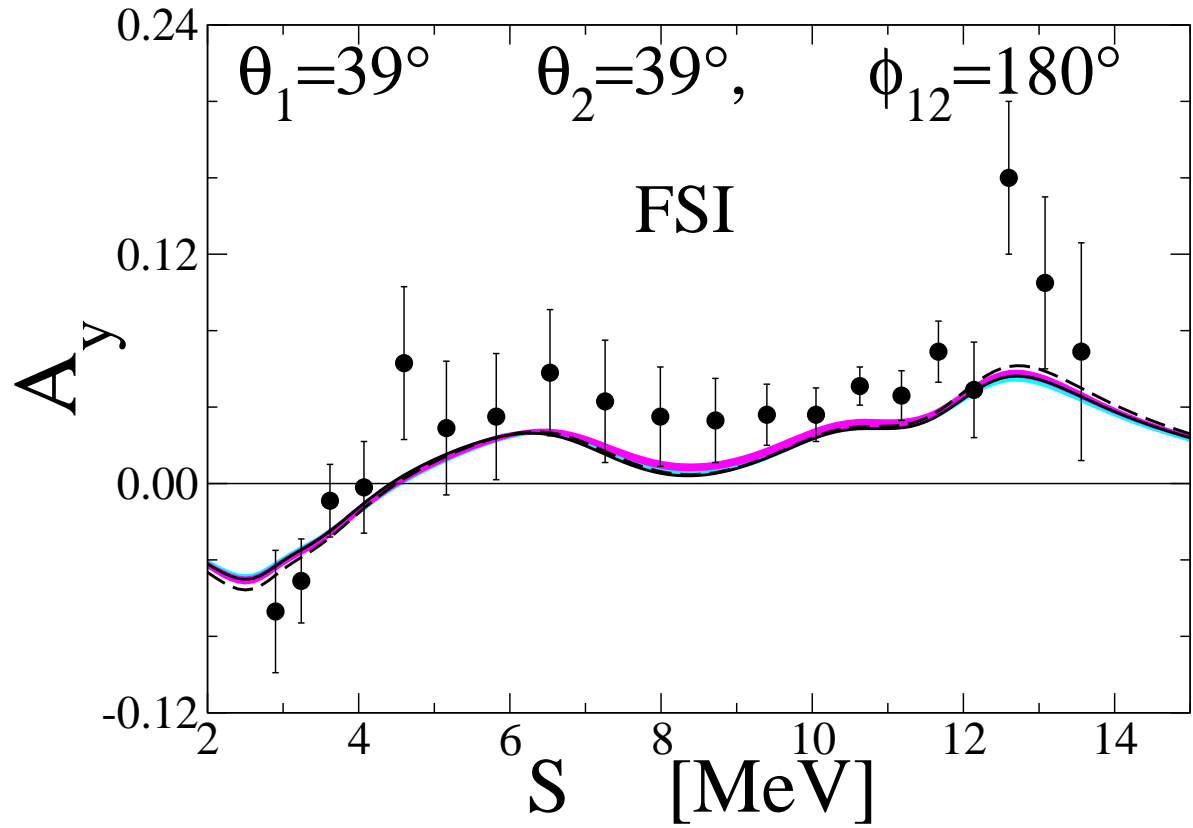


FIG. 10. Nucleon analyzing power A_y data in Nd breakup at 13 MeV in comparison to theory. Bands and curves as in Fig. 1. The pd data are from [28].

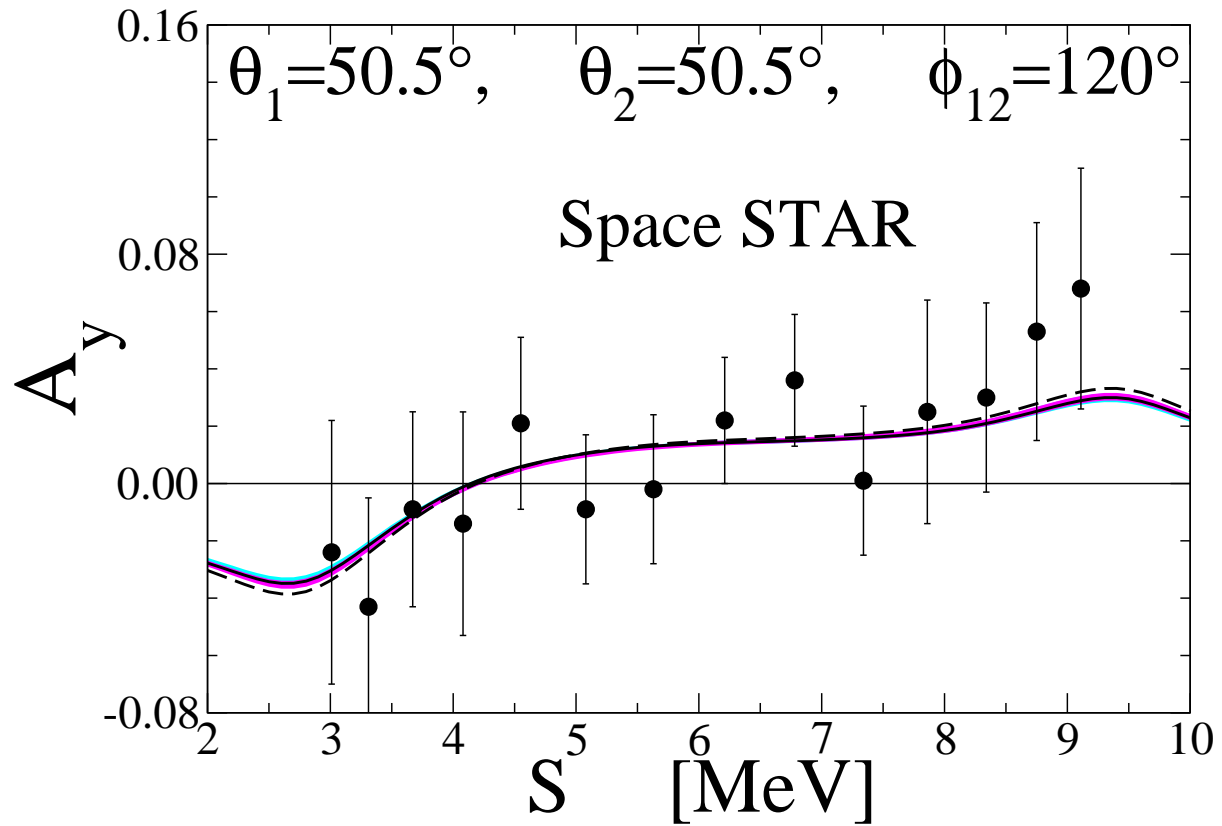


FIG. 11. Nucleon analyzing power A_y data in Nd breakup at 13 MeV in comparison to theory. Bands and curves as in Fig. 1. The pd data are from [28].

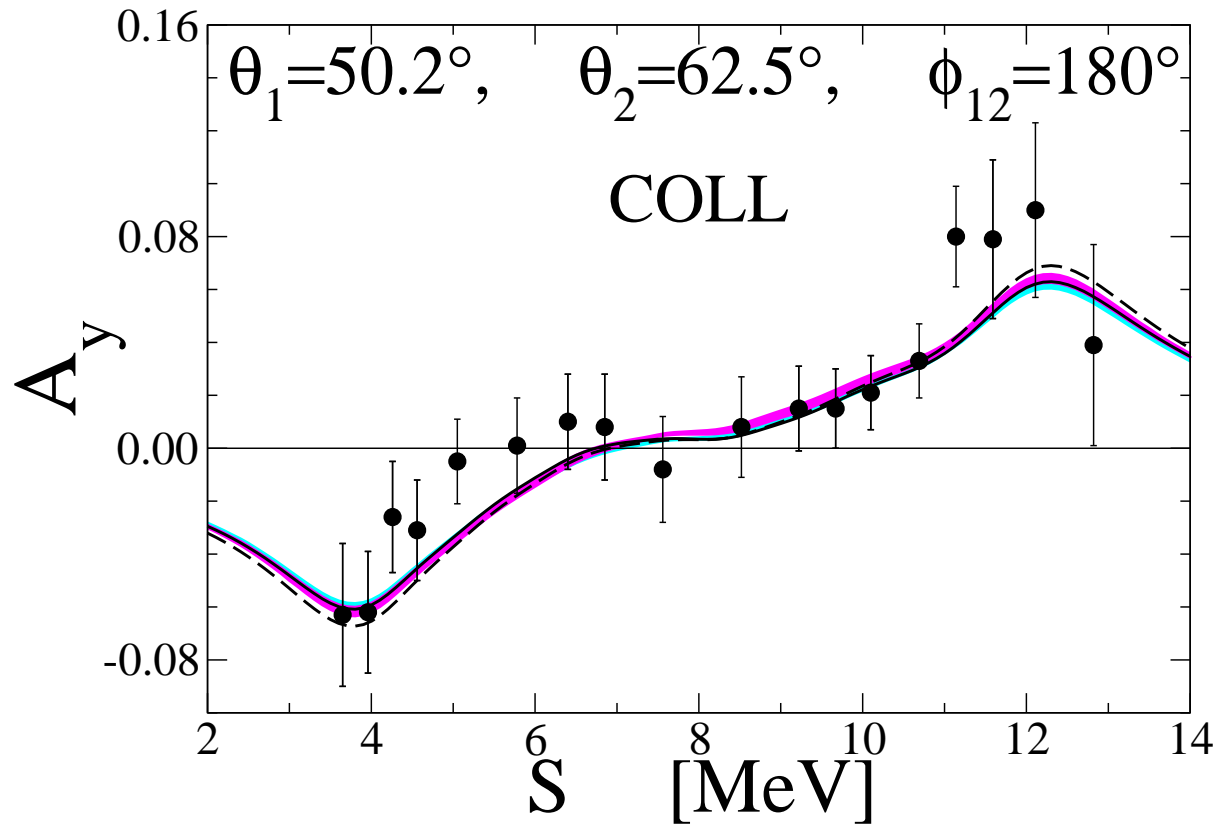


FIG. 12. Nucleon analyzing power A_y data in Nd breakup at 13 MeV in comparison to theory. Bands and curves as in Fig. 1. The pd data are from [28].

FIG. 13. Nd breakup cross section in $[\text{mb MeV}^{-1}\text{sr}^{-2}]$ and nucleon analyzing power data at 65 MeV in comparison to theory. Symmetric space star (SSS) configuration is shown. Bands and curves as in Fig. 1. The pd data are from [40].

FIG. 14. Nd breakup cross section in $[\text{mb MeV}^{-1}\text{sr}^{-2}]$ and nucleon analyzing power data at 65 MeV in comparison to theory. Symmetric forward star (FPS) configuration is shown. Bands and curves as in Fig. 1. The pd data are from [40].

FIG. 15. Nd breakup cross section in $[\text{mb MeV}^{-1}\text{sr}^{-2}]$ and nucleon analyzing power data at 65 MeV in comparison to theory. Backward plane star (BPS) configuration is shown. Bands and curves as in Fig. 1. The pd data are from [40].

FIG. 16. Nd breakup cross section in $[\text{mb MeV}^{-1}\text{sr}^{-2}]$ and nucleon analyzing power data at 65 MeV in comparison to theory. Quasi-free scattering (QFS) configuration is shown. Bands and curves as in Fig. 1. The pd data are from [40].

FIG. 17. Nd breakup cross section in $[\text{mb MeV}^{-1}\text{sr}^{-2}]$ and nucleon analyzing power data at 65 MeV in comparison to theory. Quasi-free scattering (QFS) configuration is shown. Bands and curves as in Fig. 1. The pd data are from [40].

FIG. 18. Nd breakup cross section in $[\text{mb MeV}^{-1}\text{sr}^{-2}]$ and nucleon analyzing power data at 65 MeV in comparison to theory. Collinear (COLL) configuration is shown. Bands and curves as in Fig. 1. The pd data are from [39].

FIG. 19. Nd breakup cross section in $[\text{mb MeV}^{-1}\text{sr}^{-2}]$ and nucleon analyzing power data at 65 MeV in comparison to theory. Collinear (COLL) configuration is shown. Bands and curves as in Fig. 1. The pd data are from [39].

FIG. 20. Nd breakup cross section in $[\text{mb MeV}^{-1}\text{sr}^{-2}]$ and nucleon analyzing power data at 65 MeV in comparison to theory. Collinear (COLL) configuration is shown. Bands and curves as in Fig. 1. The pd data are from [39].

FIG. 21. Nd breakup cross section in $[\text{mb MeV}^{-1}\text{sr}^{-2}]$ and nucleon analyzing power data at 65 MeV in comparison to theory. Collinear (COLL) configuration is shown. Bands and curves as in Fig. 1. The pd data are from [39].

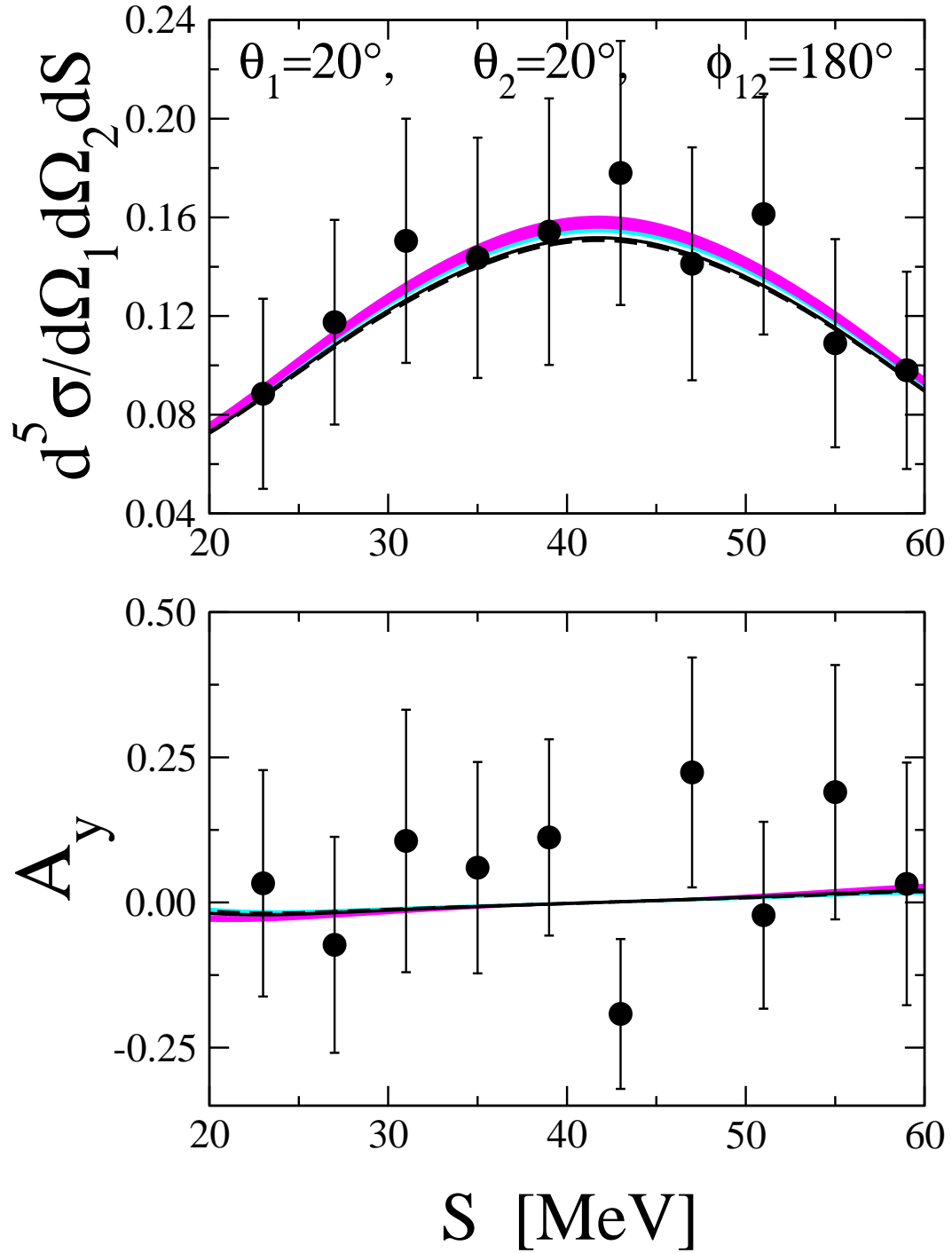


FIG. 22. Nd breakup cross section in $[\text{mb MeV}^{-1} \text{sr}^{-2}]$ and nucleon analyzing power data at 65 MeV in comparison to theory. Unspecific configuration is shown. Bands and curves as in Fig. 1. The pd data are from [41].

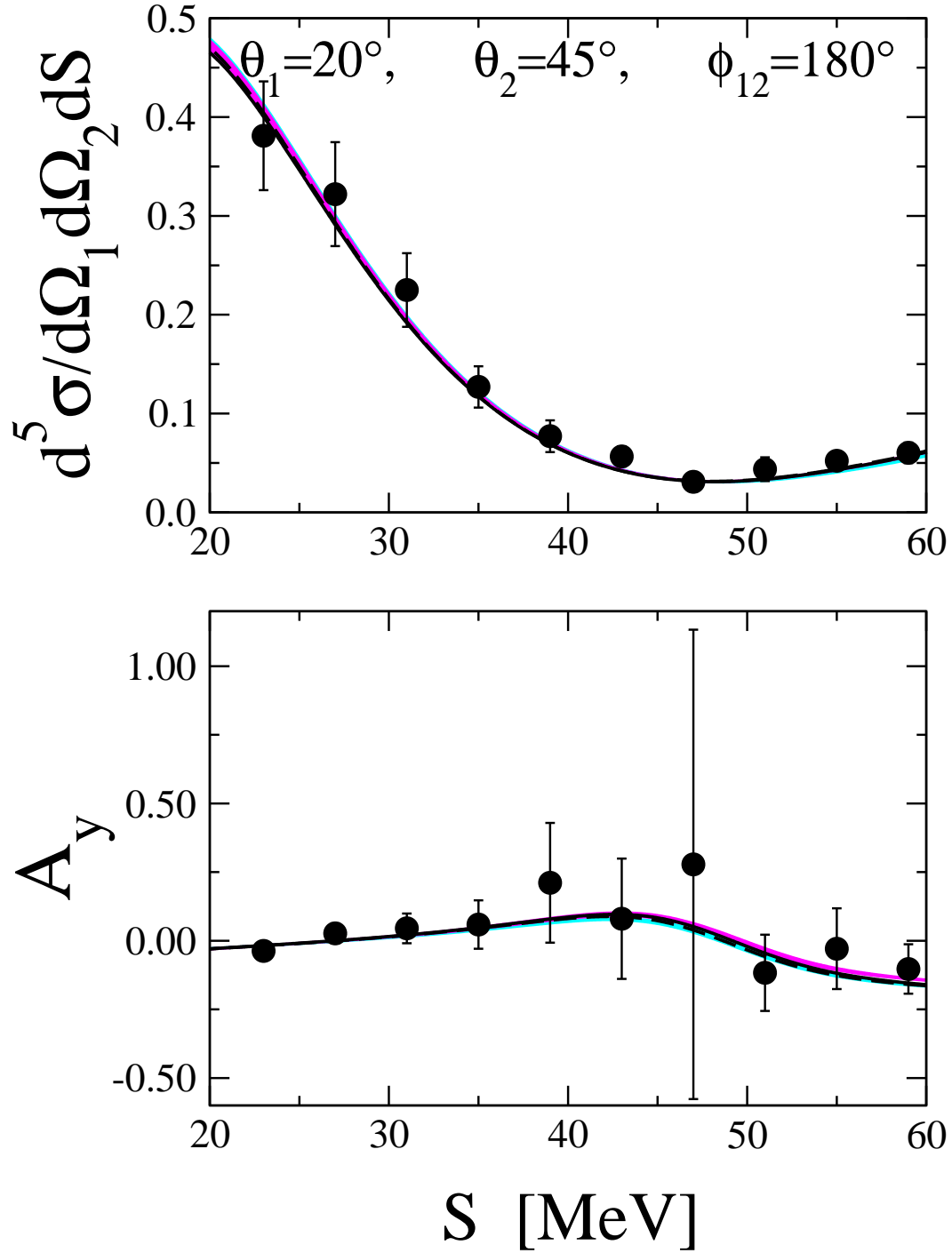


FIG. 23. Nd breakup cross section in $[\text{mb MeV}^{-1} \text{sr}^{-2}]$ and nucleon analyzing power data at 65 MeV in comparison to theory. Unspecific configuration is shown. Bands and curves as in Fig. 1. The pd data are from [41].

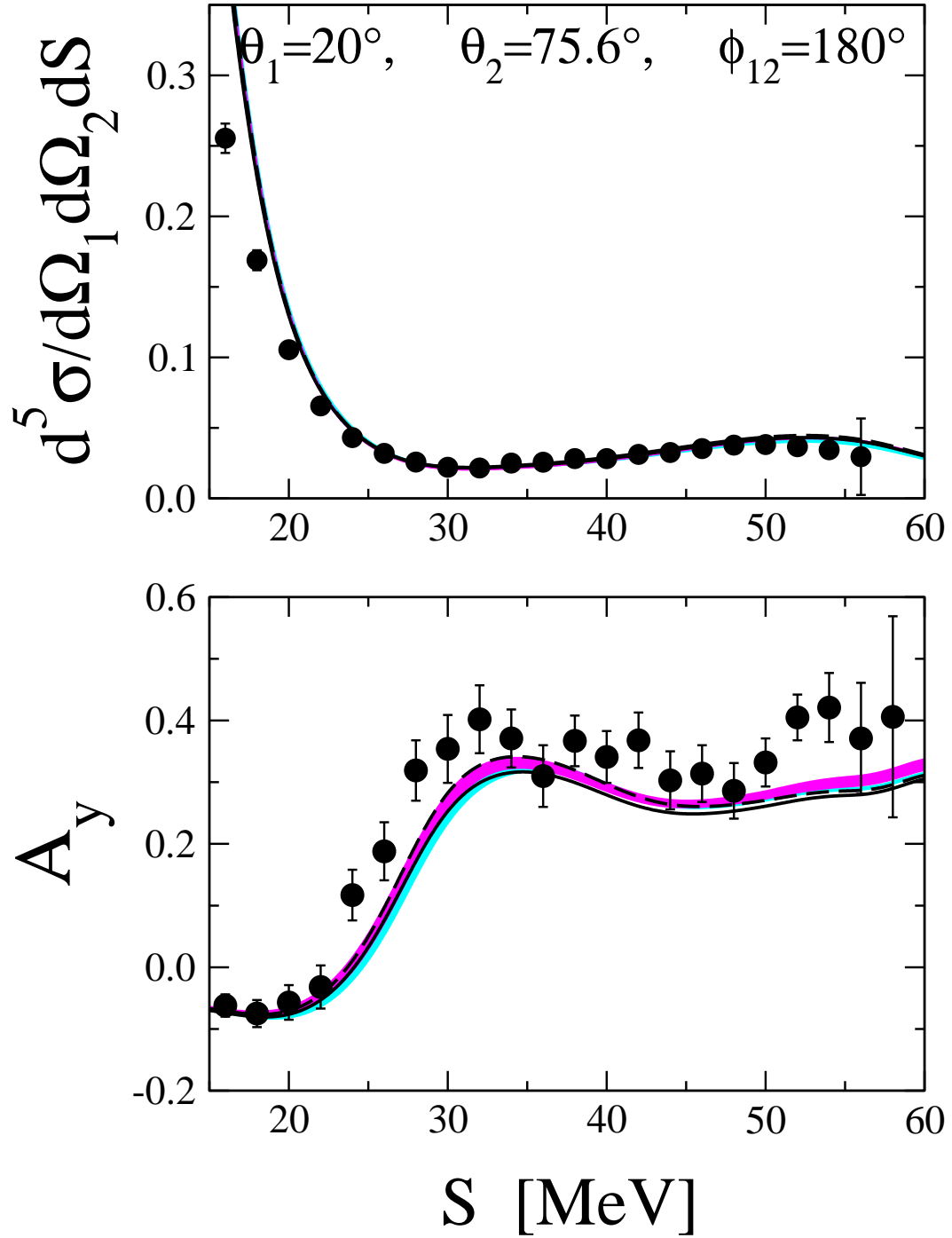


FIG. 24. Nd breakup cross section in $[\text{mb MeV}^{-1}\text{sr}^{-2}]$ and nucleon analyzing power data at 65 MeV in comparison to theory. Unspecific configuration is shown. Bands and curves as in Fig. 1. The pd data are from [41].

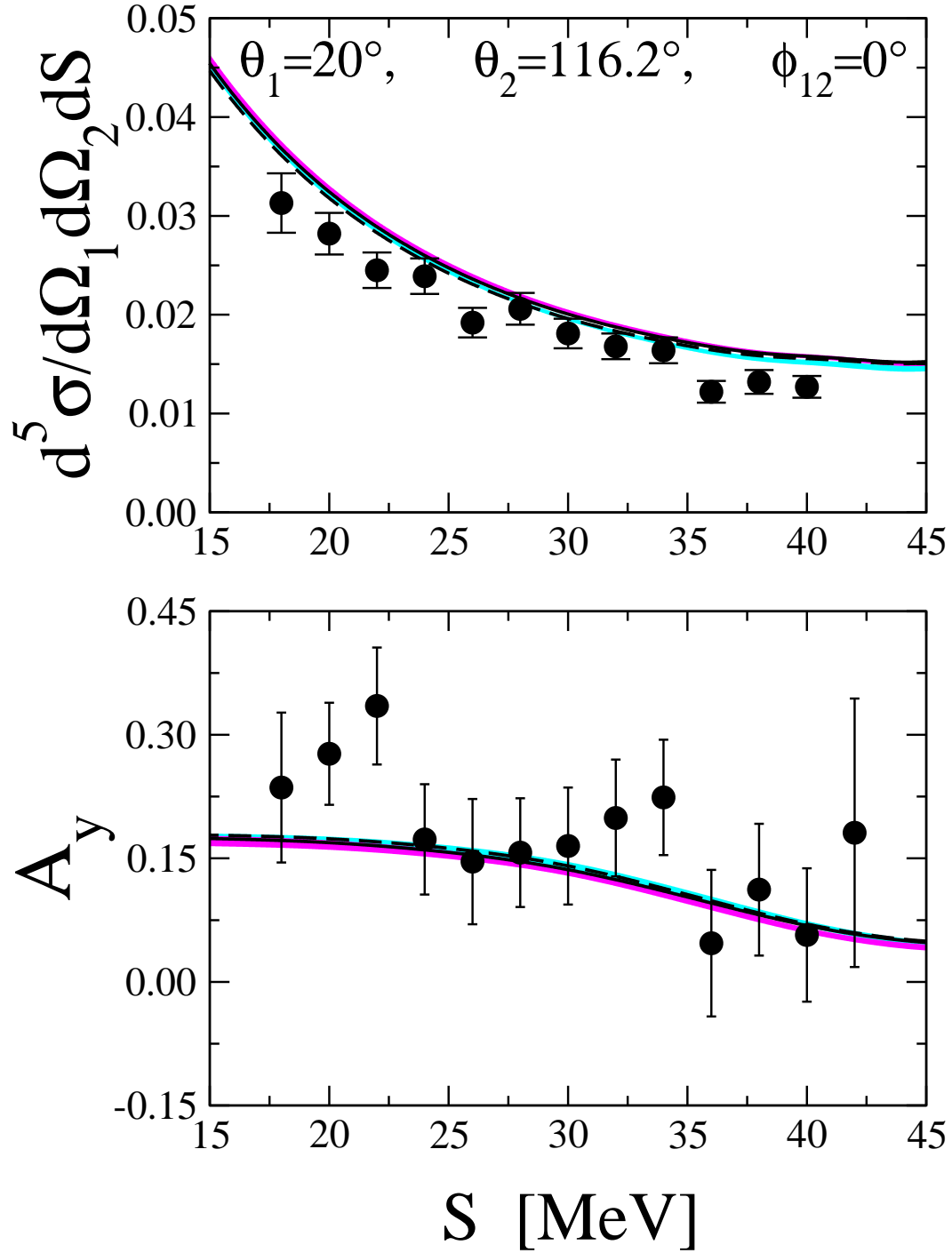


FIG. 25. Nd breakup cross section in $[\text{mb MeV}^{-1} \text{sr}^{-2}]$ and nucleon analyzing power data at 65 MeV in comparison to theory. Unspecific configuration is shown. Bands and curves as in Fig. 1. The pd data are from [41].

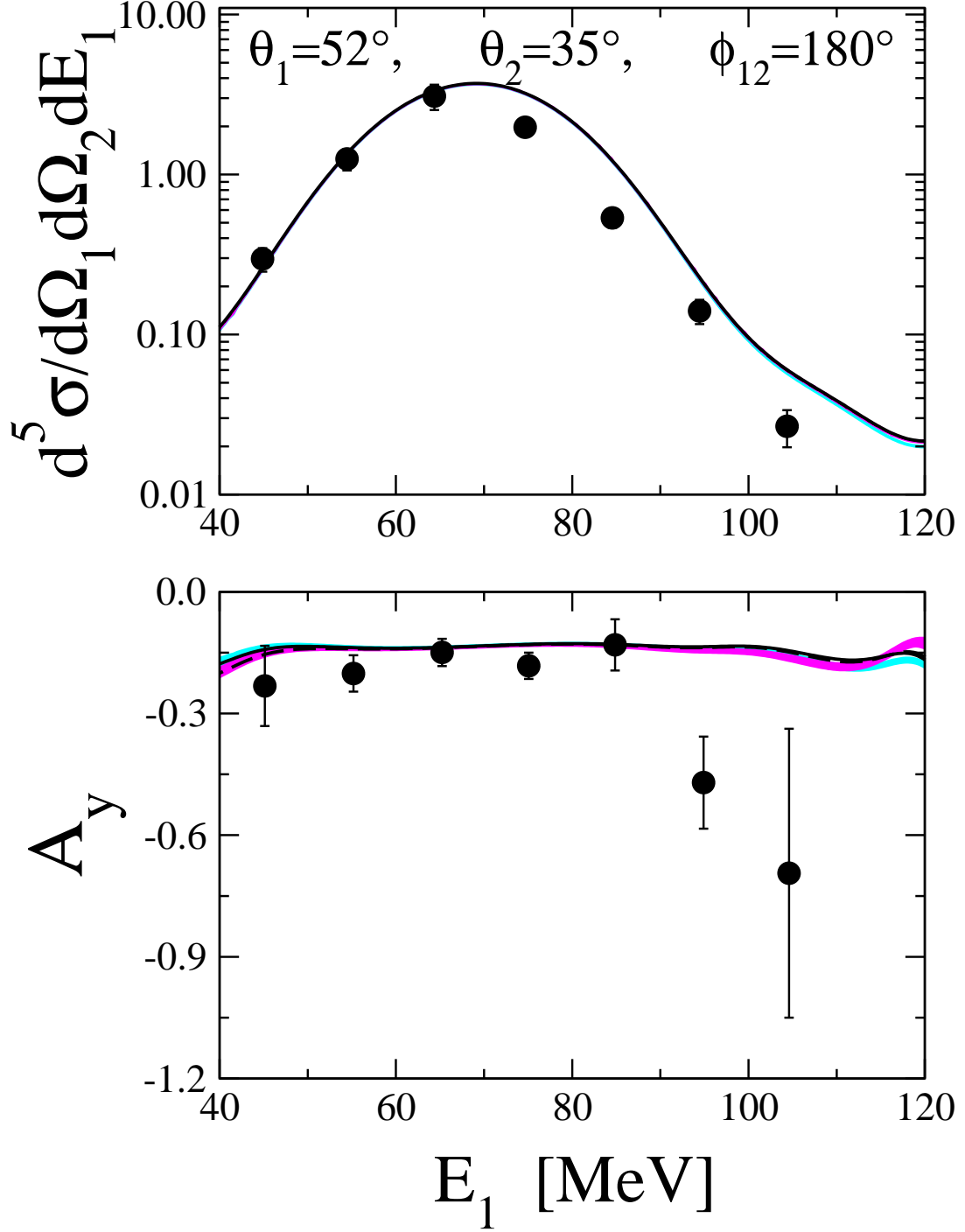


FIG. 26. Nd breakup cross section in $[\text{mb MeV}^{-1}\text{sr}^{-2}]$ and nucleon analyzing power data at 200 MeV in comparison to theory. Bands and curves as in Fig. 1. The pd data are from [17].

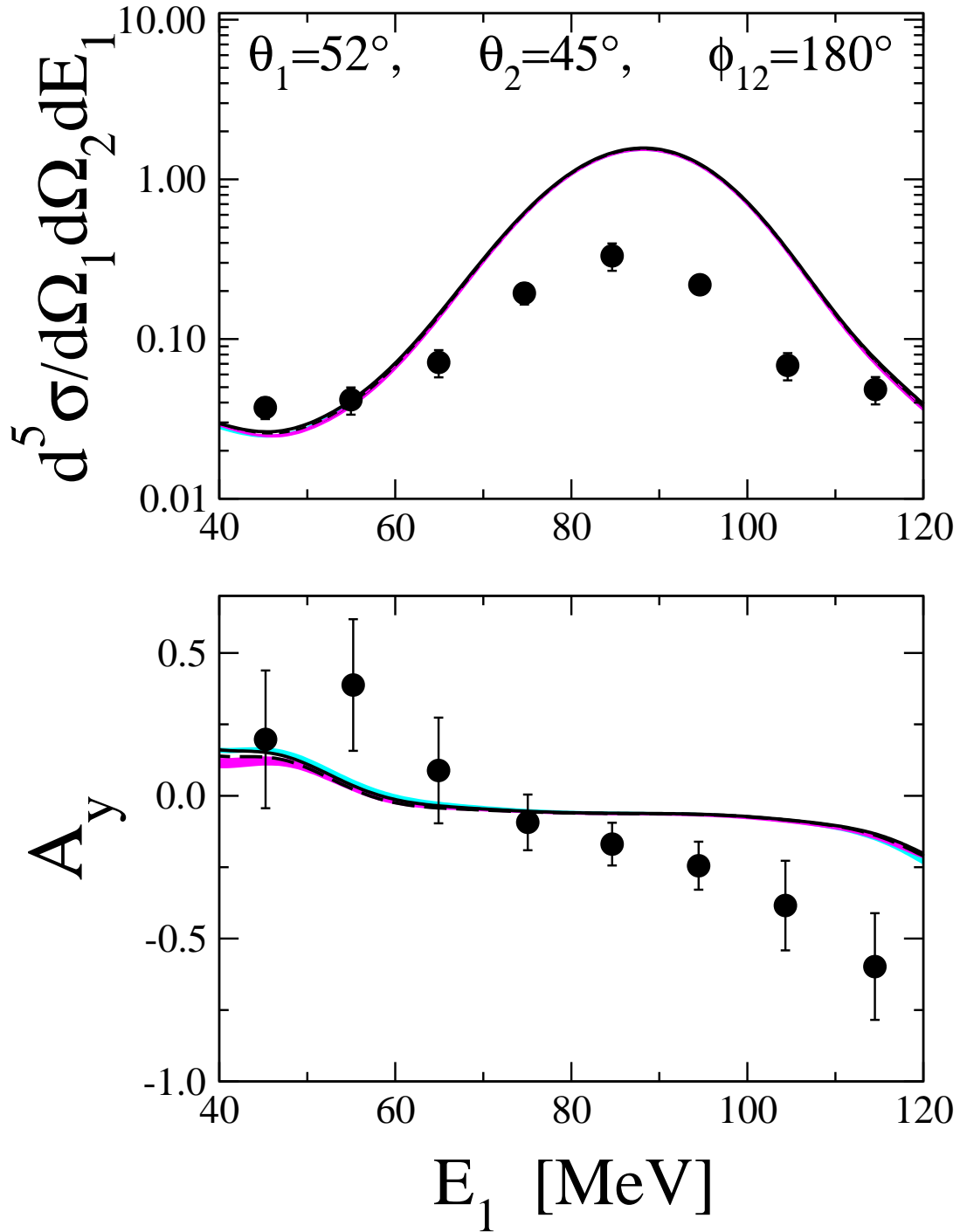


FIG. 27. Nd breakup cross section in $[\text{mb MeV}^{-1}\text{sr}^{-2}]$ and nucleon analyzing power data at 200 MeV in comparison to theory. Bands and curves as in Fig. 1. The pd data are from [17].

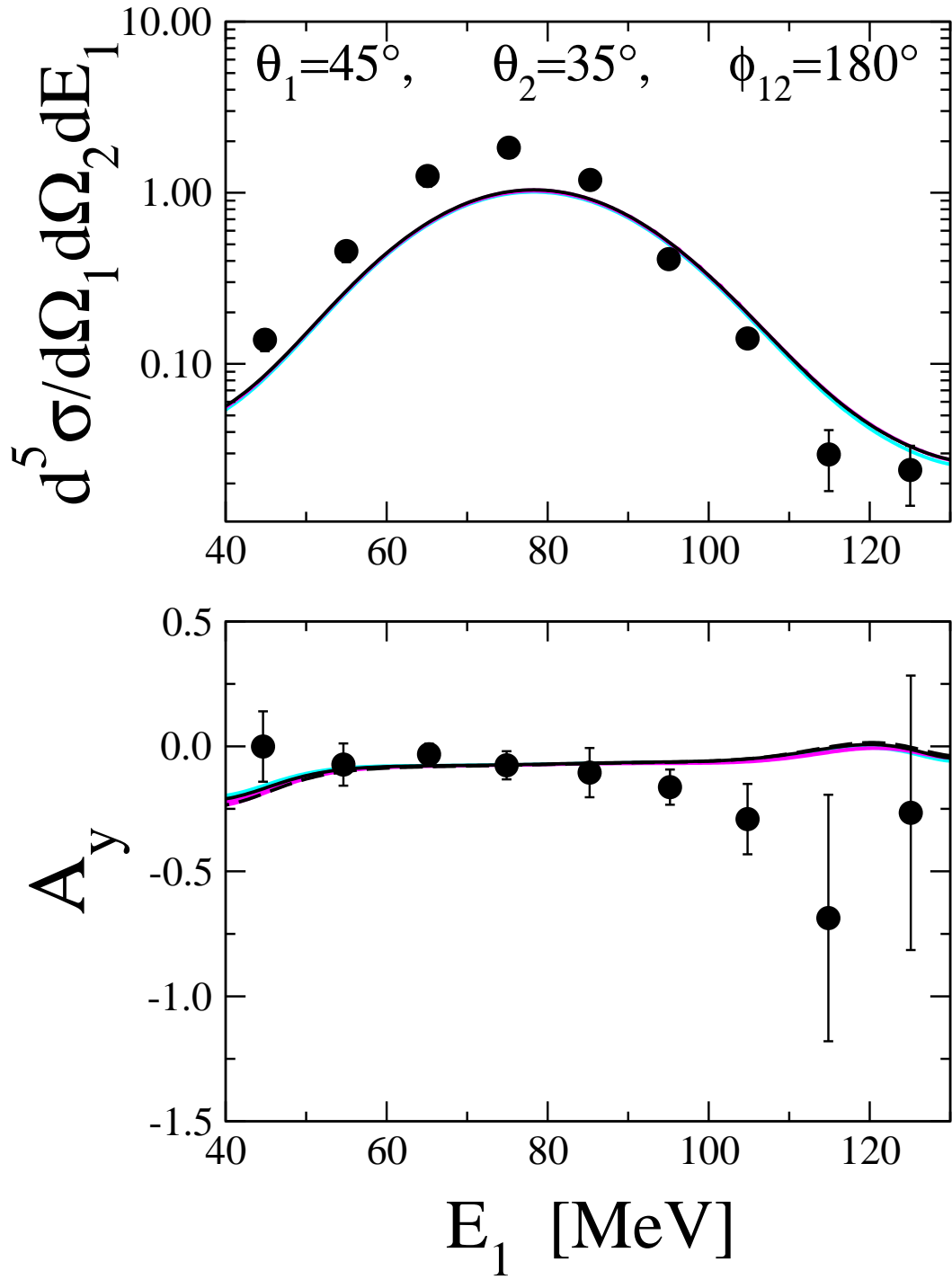


FIG. 28. Nd breakup cross section in [mb MeV⁻¹sr⁻²] and nucleon analyzing power data at 200 MeV in comparison to theory. Bands and curves as in Fig. 1. The *pd* data are from [17].

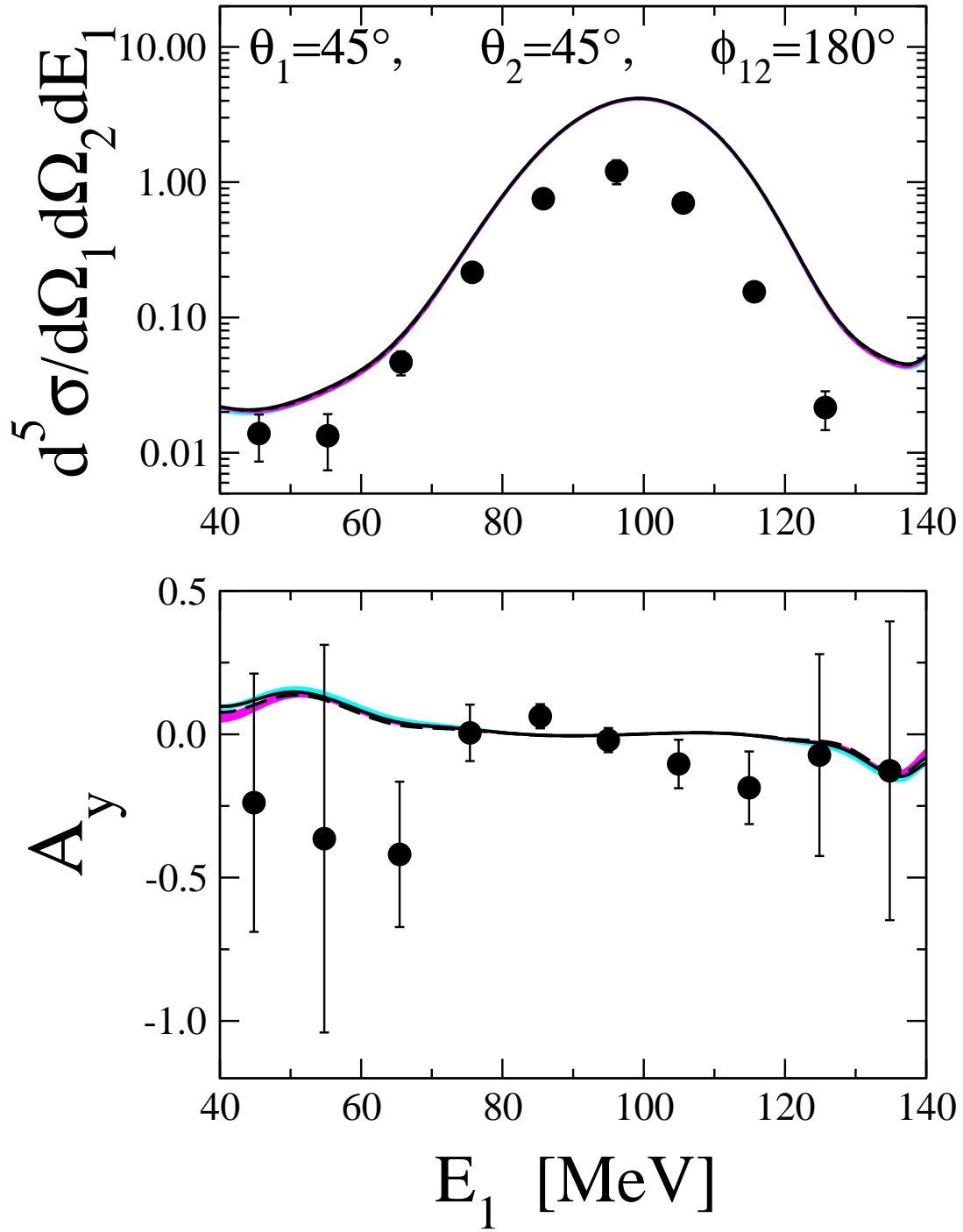


FIG. 29. Nd breakup cross section in $[\text{mb MeV}^{-1} \text{sr}^{-2}]$ and nucleon analyzing power data at 200 MeV in comparison to theory. Bands and curves as in Fig. 1. The pd data are from [17].

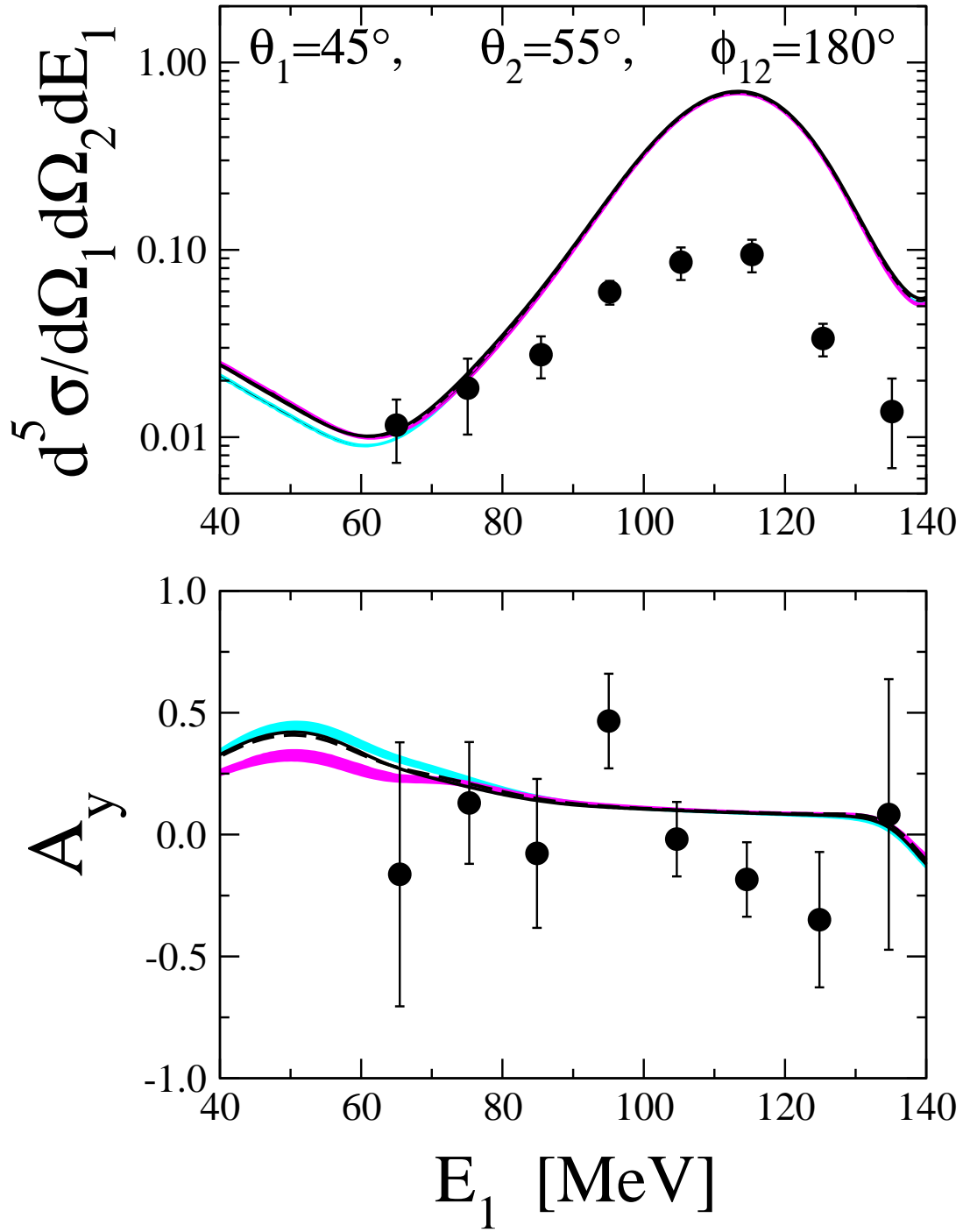


FIG. 30. Nd breakup cross section in $[\text{mb MeV}^{-1} \text{sr}^{-2}]$ and nucleon analyzing power data at 200 MeV in comparison to theory. Bands and curves as in Fig. 1. The pd data are from [17].

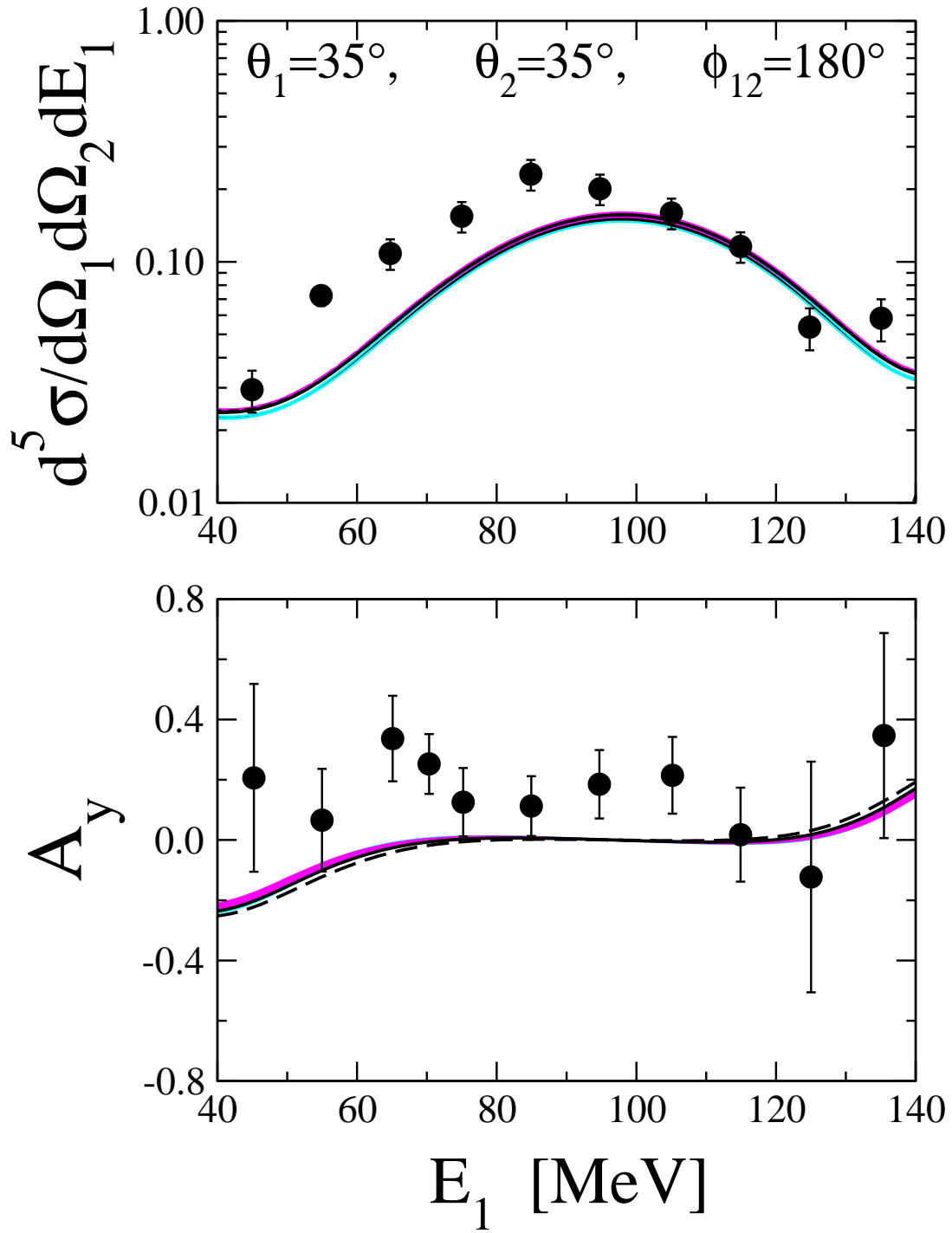


FIG. 31. Nd breakup cross section in $[\text{mb MeV}^{-1} \text{sr}^{-2}]$ and nucleon analyzing power data at 200 MeV in comparison to theory. Bands and curves as in Fig. 1. The pd data are from [17].

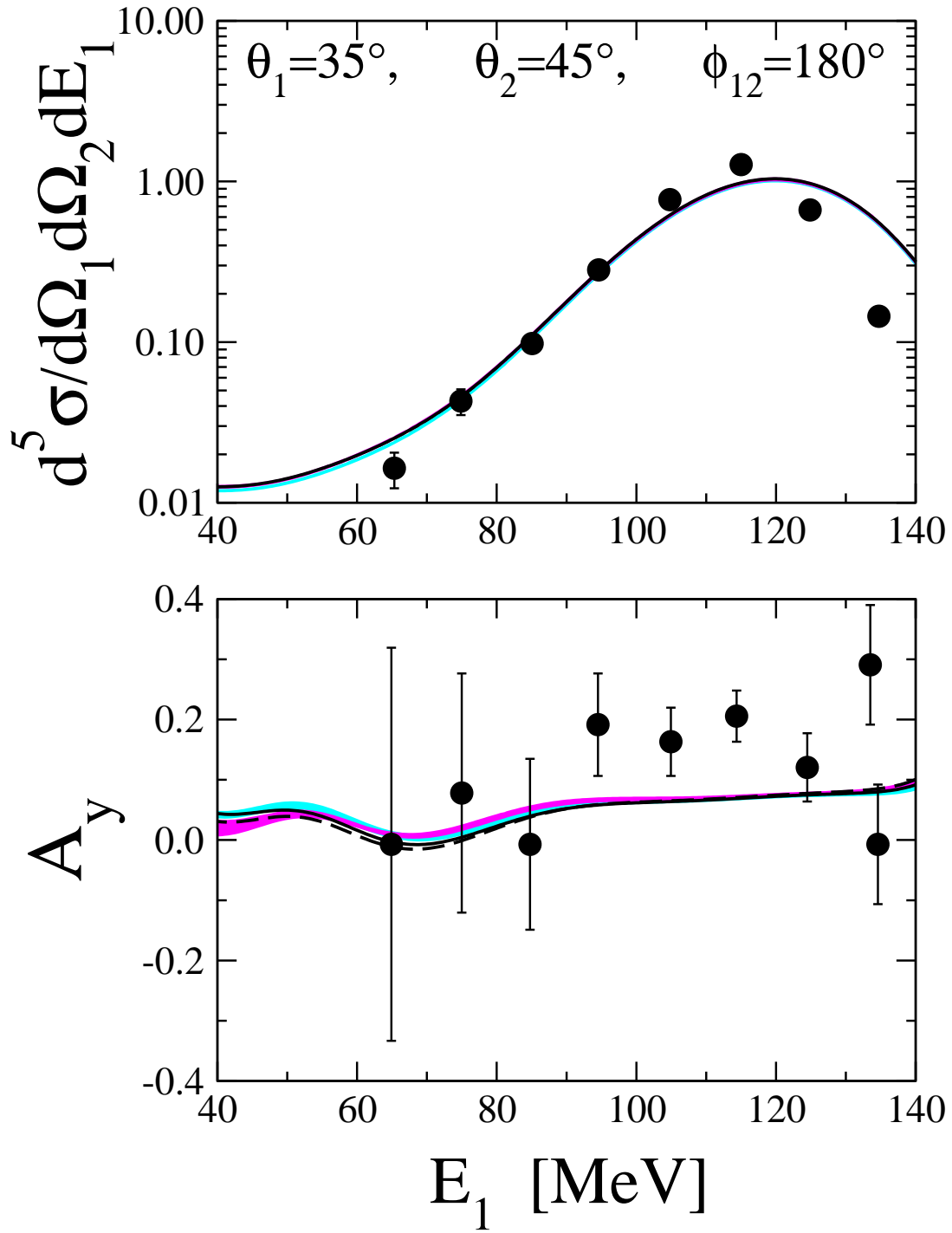


FIG. 32. Nd breakup cross section in $[\text{mb MeV}^{-1} \text{sr}^{-2}]$ and nucleon analyzing power data at 200 MeV in comparison to theory. Bands and curves as in Fig. 1. The pd data are from [17].

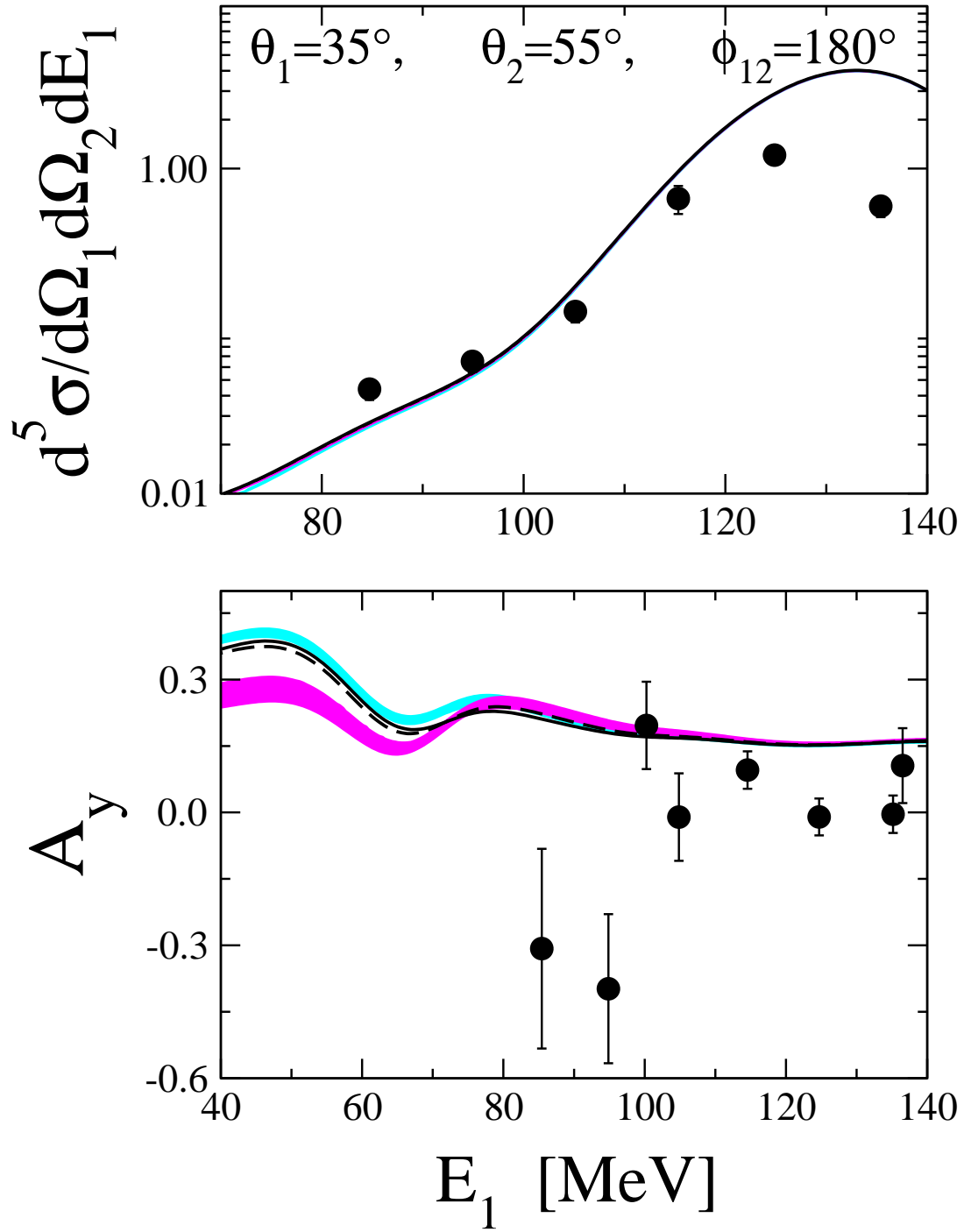


FIG. 33. Nd breakup cross section in $[\text{mb MeV}^{-1} \text{sr}^{-2}]$ and nucleon analyzing power data at 200 MeV in comparison to theory. Bands and curves as in Fig. 1. The pd data are from [17].

This figure "break_partII_fig13.gif" is available in "gif" format from:

<http://arxiv.org/ps/nucl-th/0203020v1>

This figure "break_partII_fig14.gif" is available in "gif" format from:

<http://arxiv.org/ps/nucl-th/0203020v1>

This figure "break_partII_fig15.gif" is available in "gif" format from:

<http://arxiv.org/ps/nucl-th/0203020v1>

This figure "break_partII_fig16.gif" is available in "gif" format from:

<http://arxiv.org/ps/nucl-th/0203020v1>

This figure "break_partII_fig17.gif" is available in "gif" format from:

<http://arxiv.org/ps/nucl-th/0203020v1>

This figure "break_partII_fig18.gif" is available in "gif" format from:

<http://arxiv.org/ps/nucl-th/0203020v1>

This figure "break_partII_fig19.gif" is available in "gif" format from:

<http://arxiv.org/ps/nucl-th/0203020v1>

This figure "break_partII_fig20.gif" is available in "gif" format from:

<http://arxiv.org/ps/nucl-th/0203020v1>

This figure "break_partII_fig21.gif" is available in "gif" format from:

<http://arxiv.org/ps/nucl-th/0203020v1>